

Gravity, magnetics and geothermal heat flow of the Antarctic lithospheric crust and mantle



Folker Pappa* and Jörg Ebbing

Institute of Geosciences, Kiel University, Otto-Hahn-Platz 1, D-24118, Kiel, Germany

FP, 0000-0002-5170-4919; JE, 0000-0001-7492-5338

*Correspondence: folker.pappa@ifg.uni-kiel.de

Abstract: This chapter describes the application and coverage of gravity and magnetic data for Antarctica with emphasis on airborne and satellite models. Low resolution satellite data help to fill gaps between high-resolution airborne data. Satellite gravity data are best used to study broad-scale lithospheric architecture while airborne data, especially magnetic data, provide finer detail. We review examples of gravity and magnetic analysis and describe the possibilities and pitfalls for estimating the properties of the lithosphere as it relates to the mantle. This is followed by a discussion on geothermal heat flow and possible ways to combine different geophysical and petrological models for a better understanding of the Antarctic mantle.

Antarctica, despite its remoteness and size, has been the focus of systematic geophysical data acquisition from as early as the International Geophysical Year 1957–58. A wealth of modern airborne geophysical surveys, including airborne gravimetry and magnetics over largely unexplored Antarctic frontiers, such as the Gamburtsev Subglacial Mountains (Bell *et al.* 2011; Ferraccioli *et al.* 2011) and Wilkes Land in East Antarctica (Aitken *et al.* 2014) was stimulated by the International Polar Year 2007/2008 (Krupnik *et al.* 2011). Because of these efforts, more than two-thirds of the continent has been covered by airborne surveys, albeit with varying resolution and data quality, which is a challenge for data compilations.

Nevertheless, the first modern Antarctic-wide gravity data compilation was derived from 13 million data points and covered an area of 10 million km², which corresponds to 73% coverage of the continent (Scheinert *et al.* 2016). The first Antarctic magnetic anomaly compilation (ADMAP-1) was produced in 2001 from more than 1.5 million line-km of shipborne and airborne measurements (Golynsky *et al.* 2001), succeeded in 2018 by the second-generation Antarctic magnetic anomaly compilation (ADMAP-2) including now more than 3.5 million line-km of aeromagnetic and marine magnetic data that more than doubles the initial near-surface database (Golynsky *et al.* 2018).

Still, gaps in survey coverage exist, especially in the interior of the continent and satellite data can be used to fill these gaps. A number of missions (CHAMP, GRACE, GOCE, Swarm) have been launched by international agencies since the beginning of the century that begin to fill the gap between airborne data and earlier satellite data and which can be used to study the crust and upper mantle over the entire continent.

The applications of gravity and magnetic data are many and span from estimating variations in ice thickness or depth to the top of the crystalline basement, mapping geological units, the depth of the Moho boundary, to modelling the lithosphere thickness. Along with petrological studies, gravity and magnetic data can inform us about the thermal structure and composition of the lithosphere.

Geothermal heat flow at the base lithosphere is often interpreted from the 1300-degree isotherm (Eaton *et al.* 2009), with variable radiogenic heat-production in the crust related to rock type. To date, only a few direct estimates of geothermal heat flow are available over Antarctica, making geophysical models useful proxies that often rely on magnetic or gravity derived models, or a combination of those, with seismological results.

This chapter will provide a summary of gravity and magnetic data, discuss some applications of these data to understand the mantle and lithosphere, and provide a brief

discussion of the state of the art with respect to geothermal heat flow estimates from geophysical models.

Gravity

Gravity observations in Antarctica: scales and strides

Gravity data allow detection and interpretation of subsurface structures related to density variations. Such features can, for instance, be subglacial or submarine troughs, sedimentary basins, sub-glacial volcanoes, intrusions, tectonic suture zones, the depth of the crust–mantle boundary (Moho discontinuity), or mantle density variations. The commonly used products for interpretation are the free-air gravity anomaly, the Bouguer gravity anomaly or the isostatic anomaly. Measured data are corrected for the station height and Earth's normal gravity, which also considers its ellipticity, which results in the free-air anomaly. If in addition the effects induced by topographic features with a constant standard rock density (2670 kg m⁻³) are removed, one obtains the Bouguer gravity anomaly, which reveals density inhomogeneities in the subsurface (e.g. Nowell 1999). Typical example are the crustal roots under mountain chains that isostatically compensate topography. With additional information about subsurface density structures that are relevant for the isostatic behaviour of the solid Earth, one can compute their effect on the gravity field, which is referred to as the isostatic correction (e.g. Kaban *et al.* 2004). After applying the isostatic correction to the Bouguer gravity anomaly, the resulting isostatic residual anomaly reveals deviations of the Earth from the state of isostatic equilibrium.

Gravimetric measurements can be taken on the ground with high precision, but require considerable logistical effort for remote regions to cover small areas relative to the size of the Antarctic continent. Therefore, mostly airborne and satellite surveys are acquired for Antarctica. In recent years, considerable progress has been made in both global Earth gravity field observations by satellite missions and regional airborne campaigns (e.g. Ferraccioli *et al.* 2011; Riedel *et al.* 2012; Aitken *et al.* 2014; Scheinert *et al.* 2016; Forsberg *et al.* 2018). The lateral resolution of these two techniques ranges from 130 to 80 km for static gravity models derived from satellite data (Mayer-Gürr *et al.* 2010, 2012) to less than 10 km for airborne data (e.g. Forsberg *et al.* 2011). Long-wavelength satellite data are particularly useful to study the deeper lithospheric and sub-lithospheric upper mantle structures. Aerogravimetry compilations often lack such information due to post-processing

and combination procedures of individual flight lines and thus focus on small-scale and shallow features. Theoretically, the maximum wavelength detectable by airborne measurements is half the extent of the surveyed area, but it is often shorter due to processing steps such as levelling (e.g. Barzaghi *et al.* 2014). Aerogravimetric and satellite data are therefore combined in Earth gravitational models, in order to achieve a high degree of consistency together with high resolution where data are available (e.g. Forsberg 2015; Pail *et al.* 2018).

The twin-satellite mission GRACE (Gravity Recovery and Climate Experiment), orbiting Earth at *c.* 450 km height from 2002 to 2017, did not only measure the long wavelength signal of the gravitational field with high precision (Tapley *et al.* 2004) but also allowed us to track changes over time. In the years 2009–13 the complementary GOCE (Gravity field and steady-state Ocean Circulation Explorer) satellite mission mapped the gravity gradient field of the Earth at *c.* 255 km altitude (*c.* 225 km in the final stage) with its three-dimensional gradiometer (Rummel *et al.* 2011; Bouman *et al.* 2015). The gravity gradients are the second derivative of the gravitational potential, also known as the Marussi Tensor, consisting of six unique components. While the spatial resolution could be

improved significantly to *c.* 80 km, GOCE's gravity gradient measurement has a poorer sensitivity at long wavelengths, which is why global Earth gravity models often combine GRACE and GOCE data to exploit the complementary advantages (e.g. Peidou and Pagiatakis 2019; Zingerle *et al.* 2019). Due to the orbit inclination, however, both satellite missions do not cover the entire Earth, which means that data gaps at the poles exist. In the case of GRACE, the observations extend to 89° (Reigber 2006), whereas for GOCE the polar gap covers regions beyond 83.5° S (Forsberg *et al.* 2011; Brockmann *et al.* 2014) and is as large as 1400 km in diameter (Scheinert *et al.* 2016). Recent efforts have been made in the course of the PolarGAP initiative to fill the gap with extensive airborne gravity measurements (Forsberg 2015).

Great advances have also been made in collecting and compiling airborne gravimetric data for the Antarctic continent and its adjacent oceanic areas. The AntGG compilation (Scheinert *et al.* 2016) covers 73% of Antarctica with a 10 km resolution grid and provides free-air and Bouguer gravity anomaly estimates (Fig. 1). Remaining gaps like the interior of Dronning Maud Land are being successively filled by additional surveys, which reveal unexplored geological features, help to

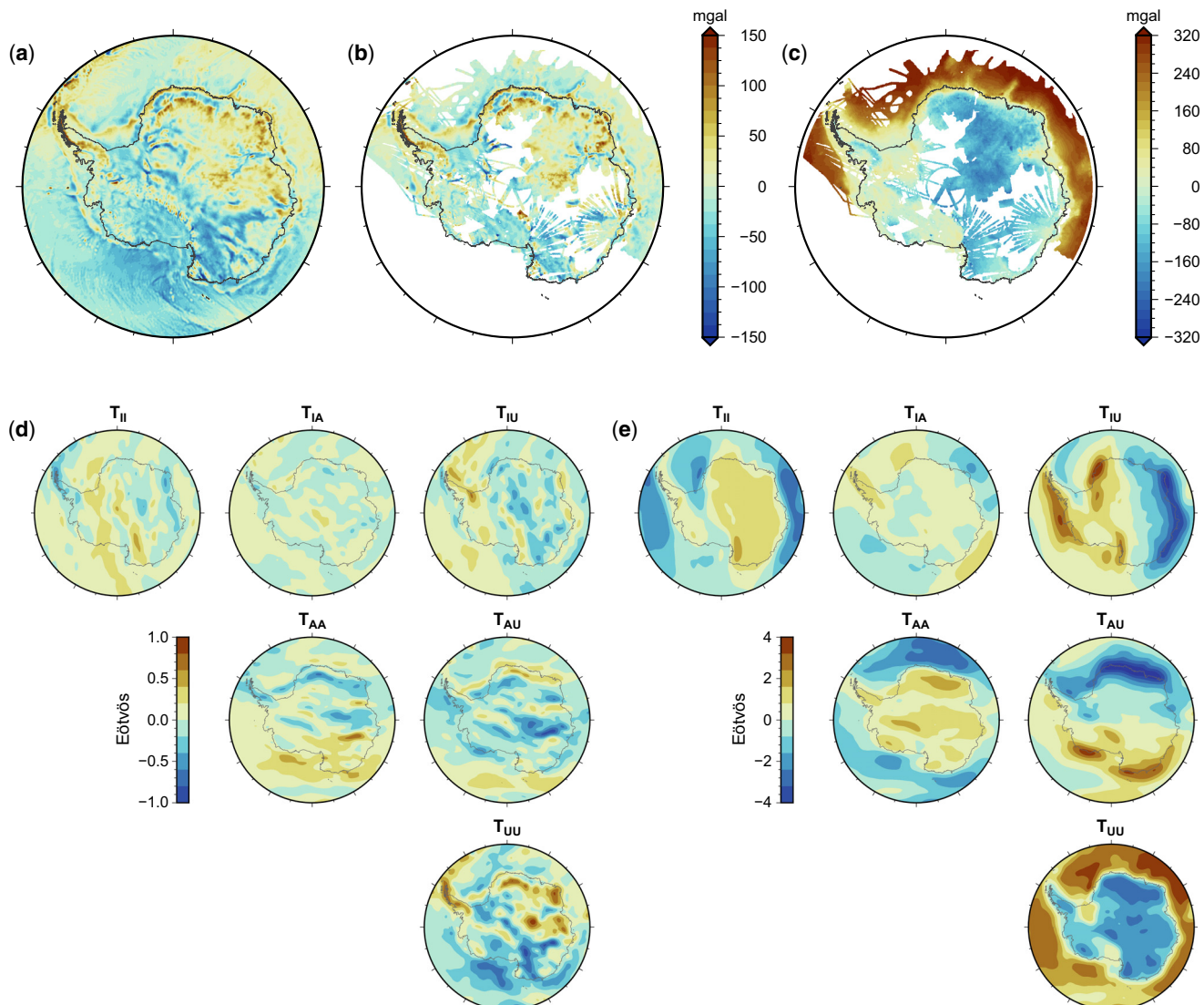


Fig. 1. Gravity data of Antarctica: (a) gravity anomaly of combined satellite model XGM2016 (Pail *et al.* 2018), (b) free-air and (c) Bouguer gravity anomalies from airborne survey data (Scheinert *et al.* 2016), (d) gravity gradient components from GOCE data (Bouman *et al.* 2016) at satellite altitude (225 km) and (e) topography-corrected gravity gradients. Gravity gradients are expressed in the IAU reference frame (Pappa *et al.* 2019b) with axes pointing to the Indian Ocean (I), Atlantic Ocean (A), and upward (U) direction.

Interpretation and modelling of geophysical data

evaluate existing gravity models, or solely confirm vintage data (Jordan *et al.* 2017; Yildiz *et al.* 2017; Forsberg *et al.* 2018). With the picture of Antarctica's gravitational signal getting successively clearer and more complete, large-scale tectonic features and crustal structures can be studied on a more robust basis. Furthermore, gravitational signatures can, together with other data like magnetic measurements, identify or assure the links between the Antarctic and its adjacent continents within the Gondwana, Rodinia and Columbia supercontinents (Aitken *et al.* 2016; Scheinert *et al.* 2016).

The Shape index: a gravitational field curvature product to study the lithospheric structure

Since satellite gravity measurements provide homogeneous data coverage over nearly the entire globe, one can search for similar characteristics in the gravitational field between regions in Antarctica and those in better-studied continents. Gravity gradients as measured by GOCE (Fig. 1) are particularly suited for this purpose due to their high sensitivity to

density variations in lithospheric depth ranges (Bouman *et al.* 2016). In modelling of gravity gradients, the individual depth sensitivity of each gradient component can be used to support the modelling effort. For interpretation, it is, however, challenging to use multiple gravity gradient components simultaneously. Combining the gravity gradient components can simplify the interpretation and thus be of use for the broad scientific community.

An example of a gravity (gradient) data product that can be interpreted relatively easily is the shape index. Hereby, the gravity gradient tensor, is translated into an index value ranging from -1 for a bowl-like shape of the equipotential surface to $+1$ for a dome-like shape, which can be interpreted in terms of characteristics of the continental lithosphere. Ebbing *et al.* (2018) applied this technique on GOCE's global gravity gradient data after correcting them for topographic effects. The shape index indicates mass deficits in the lithosphere with negative values (bowls) and mass surplus with positive values (domes) and thus enhances lithospheric and intra-crustal density variations. In the global view (Fig. 2a), bowls can generally be correlated with cratonic areas or orogenic belts, e.g. the Kaapvaal Craton in South Africa and the Himalayas. In these

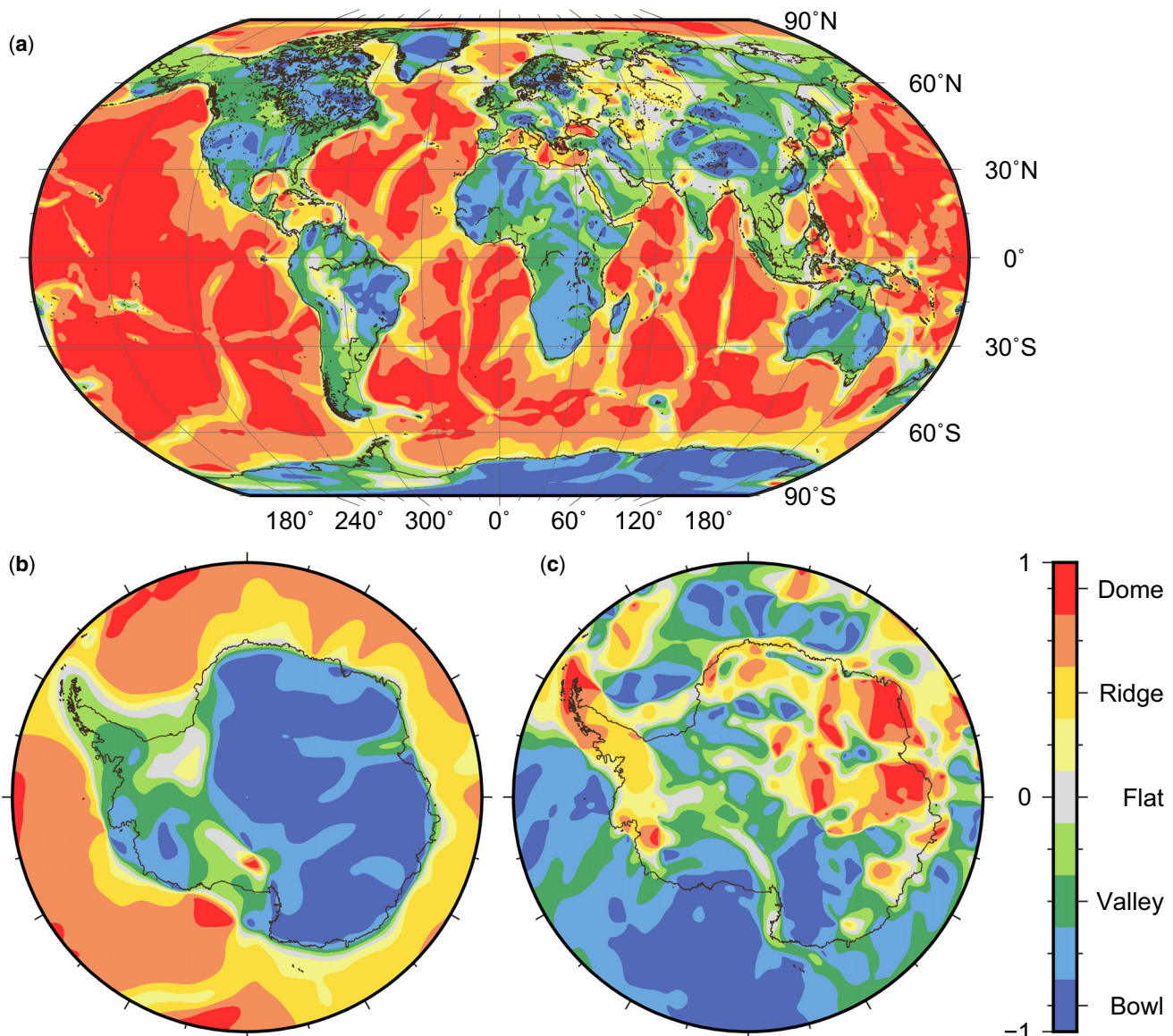


Fig. 2. Shape index based on GOCE gravity gradient data after topographic correction for (a) the Earth and (b) Antarctica (based on Ebbing *et al.* 2018). Panel (c) shows the shape index for Antarctica after additional correction for isostatic effects.

cases, mass deficits can be explained by depleted lithospheric mantle composition in cratonic settings and thick crustal roots beneath mountain ranges. On the other hand, the Andes exhibit a valley-like shape, most likely due to the additional masses of the cold subducted slab. Dome-like shapes indicate a positive shape index and generally correlate with oceanic lithosphere (e.g. the Pacific Ocean) and rifting (e.g. Red Sea).

In light of this global correlation, one can compare the shape index of Antarctica (Fig. 2b) with other regions of the world. A clear distinction between West Antarctica and East Antarctica is obvious, particularly pronounced through high shape index values in the West Antarctic Rift System and the Weddell Sea Rift, but also above the Antarctic Peninsula. Only Marie Byrd Land exhibits a bowl-like shape in West Antarctica. Underneath this region, a Cenozoic mantle plume has been proposed (LeMasurier and Rex 1989), which would likely imply relatively low densities of the upper mantle due to elevated temperatures. Independently observed low seismic velocities have been interpreted as a result of such a thermal anomaly (e.g. Lloyd *et al.* 2015; Wiens this volume, *in review*). The shape index can neither confirm nor disprove the existence of a mantle plume, but it is consistent with a thermal anomaly at depth (see Bredow and Steinberger (2021, this volume), for an in-depth discussion of the possible mantle plume).

East Antarctica, on the other hand, shows entirely negative shape index values, comparable to those of other cratonic regions on Earth. Here, the Lambert Graben stands out with an almost flat shape index, which likely reflects the tectonic setting of a failed rift system (e.g. Harrowfield *et al.* 2005). In addition to a topographic correction, the gravitational field can be reduced for isostatic effects in order to bring out the isostatic state. Figure 2c shows the shape index for Antarctica after applying a topographic reduction and subtracting the effect of an isostatically compensated Moho. The patterns are generally similar to the observed gravity anomaly (Fig. 1), though some differences can be identified. For instance, the Marie Byrd Land dome and the Antarctic Peninsula are more pronounced in the shape index. The Transantarctic Mountains, on the other hand, show a flat shape index, whereas their gravity anomaly is distinctly positive with more than 50 mGal. This can be interpreted as an expression of a missing crustal root beneath the Transantarctic Mountains (e.g. Hansen *et al.* 2016) and their still unresolved isostatic state and uplift history (e.g. Lisker *et al.* 2013).

Elastic lithosphere

Using a flexural uplift model, Stern and ten Brink (1989) early on could explain the apparent contradiction of a missing root under and the persistence of topography of the Transantarctic Mountains. Later studies used flexural uplift to study the architecture of the Ross Sea basin (Karner *et al.* 2005) or the interaction of the Wilkes basin and Transantarctic Mountains (Paxman *et al.* 2019a).

In a flexural uplift model, or regional isostasy, in comparison to conventional Airy or Pratt-isostasy, the elastic properties of the lithosphere are taken into account (e.g. Watts 2001). Hereby, in the simplest form, the load by the topography suppresses the elastic plate and the response is governed by the flexural rigidity of the plate. For simplicity, the flexural rigidity is often expressed by the effective elastic thickness that under the assumption of certain rheological parameters, describes the thickness of the idealized elastic plate and does not represent a physical boundary. Please note that the effective elastic thickness is not the same quantity as used in Glacial-Isostatic Adjustment modelling studies, where it describes the thickness of an idealized elastic layer.

Different techniques exist to calculate the flexural rigidity or effective elastic thickness, e.g. admittance or coherence (Watts 2001) or modifications of these (Paxman this volume). These methods all use sub-ice topography and the gravity field to derive a ratio of similarity between the two that reflects the elasticity of the lithosphere. McKenzie *et al.* (2015) or Chen *et al.* (2018) are two recent studies, that used satellite and a combined gravity model, respectively, to show that East and West Antarctica have significantly different properties. East Antarctica is generally expressed by a thick effective elastic thickness, while West Antarctica has thin effective elastic thickness. Paxman (2021, this volume) provides a comprehensive review of the elastic properties of the Antarctic continent.

Crustal thickness of Antarctica from gravity data

The Moho boundary separates crustal and mantle rocks and is, in general, associated with the most prominent density contrast in the lithosphere. Depending on the tectonic setting, the density contrast can vary between less than 200 kg m^{-3} in cratonic regions when eclogitization is involved, and more than 500 kg m^{-3} in extending basins or Phanerozoic orogens (Rabbel *et al.* 2013). Therefore, depth, geometry and density contrast at the Moho interface have a huge impact on the gravity field at a broad range of wavelengths (e.g. Sebera *et al.* 2018). Since geothermal heat flow, seismic velocities, and several other geophysical and geological parameters are strongly affected by the crustal thickness, knowledge about the Moho depth is of broad importance.

However, the observed gravity signal originates from several sources, and the free-air anomaly is largely affected by topography. In order to isolate the signal from the Moho boundary, effects from other sources, such as intra-crustal (sedimentary basins) and mantle density variations or dynamic forces as well as topography, ice and water need to be subtracted from the total signal. For Antarctica, the estimation of the sub-ice architecture is challenging. Nevertheless, huge progress has been made by establishing the Bedmap2 model (Fretwell *et al.* 2013), which describes the surface elevation, the ice thickness and the seafloor and sub-glacial bed elevation of the Antarctic and has been recently updated by the topographic model BedMachine Antarctica (Morlighem *et al.* 2020).

Since sedimentary rocks can have significantly lower densities than igneous or metamorphic rocks, it is crucial to incorporate them in a topographic reduction model. A compilation of offshore sedimentary basins in the Antarctic has recently been published (Straume *et al.* 2019), showing more than 12 km-thick sedimentary sequences in the Weddell Sea sector and up to 8 km in the Ross Sea region. The availability of data for sediment thickness is poorly constrained for onshore areas relative to offshore. Few studies exist that estimate the depth of East Antarctic inland sub-glacial basins from aerogeophysical surveys, but there are exceptions (e.g. Mishra *et al.* 1999; Bamber *et al.* 2006; Ferraccioli *et al.* 2011; Aitken *et al.* 2014; Frederick *et al.* 2016), predominantly in the Wilkes Land region, or seismic methods in Lake Vostok (Filina *et al.* 2008; Isanina *et al.* 2009) and its periphery (Studinger *et al.* 2003). It is, however, extremely challenging to establish a trustworthy model for thickness and density of East Antarctica's sedimentary basins from the available data, which would also have to account for different degrees of compaction, infill composition and age if it is supposed to be used in a gravimetric topographic reduction. In general, efforts to make sediment thickness maps of the Antarctic continent based on gravity and/or seismic estimates (e.g. Baranov *et al.* 2018; Haeger and Kaban 2019) still hold a high degree of uncertainty concerning the sediment's distribution, thickness and density.

Interpretation and modelling of geophysical data

Reasonably reliable data are currently only provided from active seismic surveys in offshore areas.

Multiple techniques exist to infer the Moho depth from gravimetric observations. The most widely used one is the Parker–Oldenburg scheme (Parker 1973; Oldenburg 1974). This approach mathematically relates the geometry of a two-dimensional interface with a vertical gravity anomaly and can thus be used to invert the inferred Bouguer anomaly of a particular region into a Moho depth model. It implies, however, a flat Earth approximation and requires presumptions of a certain (constant) density contrast and a reference depth for the Moho. Moreover, the data need to be given at Earth surface level, which means that low pass filtering and downward continuation must be performed on satellite gravity observations to prevent numerical instabilities and noise amplification. Other methods to estimate the Moho depth from the Bouguer gravity anomaly are, on the other hand, applicable in spherical coordinates and at satellite height (e.g. Moritz 1990).

Block *et al.* (2009) followed the Parker–Oldenburg approach and used GRACE satellite gravity data to estimate the crustal thickness of Antarctica, assuming a reference depth of 35 km and a density contrast of 500 kg m^{-3} . Their results showed a large contrast between the crustal thickness of West Antarctica with *c.* 30 km and East Antarctica with *c.* 40 km and a crustal root beneath the Gamburtsev Subglacial Mountains (GSM) of as much as 42 km. Seismological studies estimated the crustal thickness to be thinner (*c.* 20–30 km) in West Antarctica (e.g. Chaput *et al.* 2014; Ramirez *et al.* 2016; Shen *et al.* 2018) and much thicker (>50 km) beneath the GSM (e.g. Lawrence *et al.* 2006; Hansen *et al.* 2010; An *et al.* 2016). Even considering the rather high uncertainties of the first Bedmap model (Lythe and Vaughan 2001), the discrepancy suggests that a single density contrast and reference depth is not applicable for the whole Antarctic continent with its diverse tectonic provinces (Pappa *et al.* 2019a). Accounting for that, O’Donnell and Nyblade (2014) performed separate inversions of the Moho depth for West and East Antarctica and constrained the solutions with local seismological Moho depth estimates. Their results indicate a >50 km-thick crustal root beneath the GSM while a *c.* 23–27 km thick crust is suggested for most of West Antarctica. Integrating seismological findings in the inversion of gravity data enabled the authors to reduce the inherent ambiguity significantly. Despite these methodological improvements, however, it is still not viable to derive a Moho depth model for Antarctica from gravity with constraining seismic data (Pappa *et al.* 2019a), because the diverse tectonic regimes of the continent with different Moho density contrasts need to be accounted for. A thick and high-density crust can be similarly isostatically compensated as a thin and low-density crust. In this regard, gravity-inverted Moho depth models tend to underestimate the amplitude of crustal thickness variations.

Gravity-derived Moho depth models of Antarctica show similar morphologies because their methods are similar. In contrast to this, Moho models based solely on seismological data are notably diverse (e.g. Baranov and Morelli 2013; An *et al.* 2015b; Baranov *et al.* 2018; Haeger *et al.* 2019) and differ by more than 10 km in large areas of the continent. One reason is the variety of seismological methods applied (see also Wiens this volume, in review). Some studies suggest that S-wave receiver functions analysis is more reliable than P-wave receiver functions analysis due to the reverberation of seismic waves by the thick ice cover (e.g. Hansen *et al.* 2016). Another source for the disagreement of seismological models lies in the sparseness of seismic stations in Antarctica and the interpolation method for blank areas. Surface wave analyses can estimate the physical properties of the subsurface between seismic stations from dispersion curves, inherently

leading to smooth results with averaged values. Numerical interpolation algorithms like the Kriging method, on the other hand, fill the blank areas based on local Moho depth information in the vicinity (Baranov and Morelli 2013; Haeger *et al.* 2019; Szwilus *et al.* 2019). Both methods can differ substantially in their results, but neither of them can be declared more correct than the other.

Figure 3a–f shows six Moho depth models derived with different methods. All models show the striking contrast in crustal thickness between West Antarctica and East Antarctica as well as some prominent features with thicker crust like the GSM, the southern Transantarctic Mountains, and (with the exception of the AN1-Moho model) Marie Byrd Land. The concept of vote maps (Shephard *et al.* 2017) can be used to illustrate the degree of consistency between models and to identify common features (Fig. 3g–i). This simple method counts the number of models that match a certain criterion. All presented Moho depth models agree on a >30-km-thick crust in the whole of East Antarctica (see Fig. 3g). Likewise, large parts of West Antarctica consistently show a Moho depth shallower than 30 km, whereas the picture is diverse in the Weddell Sea region, the Antarctic Peninsula, and the vicinity of the Marie Byrd Land dome. In East Antarctica, on the other hand, only a few spots are present where at least a majority of the models exhibits a crust thicker than 40 km (Fig. 3i).

Using satellite gravity data to investigate the upper mantle structure of Antarctica

Joint interpretations of seismic findings and gravity data or isostasy (O’Donnell and Nyblade 2014; An *et al.* 2015b; Pappa *et al.* 2019a) suggest a laterally varying density contrast at the crust–mantle boundary, implying a heterogeneous upper mantle density structure beneath Antarctica. This is also indicated by seismic velocity models (e.g. Lloyd 2018). The dominating factors for both density and seismic properties of mantle rocks are temperature and composition. However, the relationships between these parameters are fundamentally different and partly non-linear or discontinuous due to mineral phase changes (e.g. Cammarano *et al.* 2003; Stixrude and Lithgow-Bertelloni 2005). For instance, the principle of isopycnicity (Jordan 1988) describes how density changes of mantle rocks due to temperatures can be compensated by opposite density changes due to compositional depletion (for discussion see also Kaban *et al.* 2003; Eaton and Perry 2013; Artemieva *et al.* 2019). Thermodynamic modelling of stable mineral assemblages (e.g. Connolly 2005) of mantle rocks under given pressure and temperature conditions can be used to establish lithospheric models that are self-consistent in terms of density, temperature and seismic velocities (e.g. Fullea *et al.* 2009, 2012). With this tool at hand, one can attempt to investigate the nature of the upper mantle of Antarctica by integrating seismological velocity models and satellite gravity data (Haeger *et al.* 2019). For this purpose, however, it is necessary to first separate the gravity signal originating from the lithospheric mantle as accurately as possible (e.g. Kaban *et al.* 2010). Hence, a crustal thickness and density model is needed, which is, as described above, subject to large uncertainties in the case of Antarctica. Haeger *et al.* (2019) used existing seismological information on Moho depth and seismic velocities in Antarctica to derive a crustal model through interpolation for a joint inversion of gravity and seismic tomography data with the aim of inferring the density, temperature, and composition of the Antarctic upper mantle. After applying the crustal correction, as described above, regions of low gravity residuals are associated with decreased

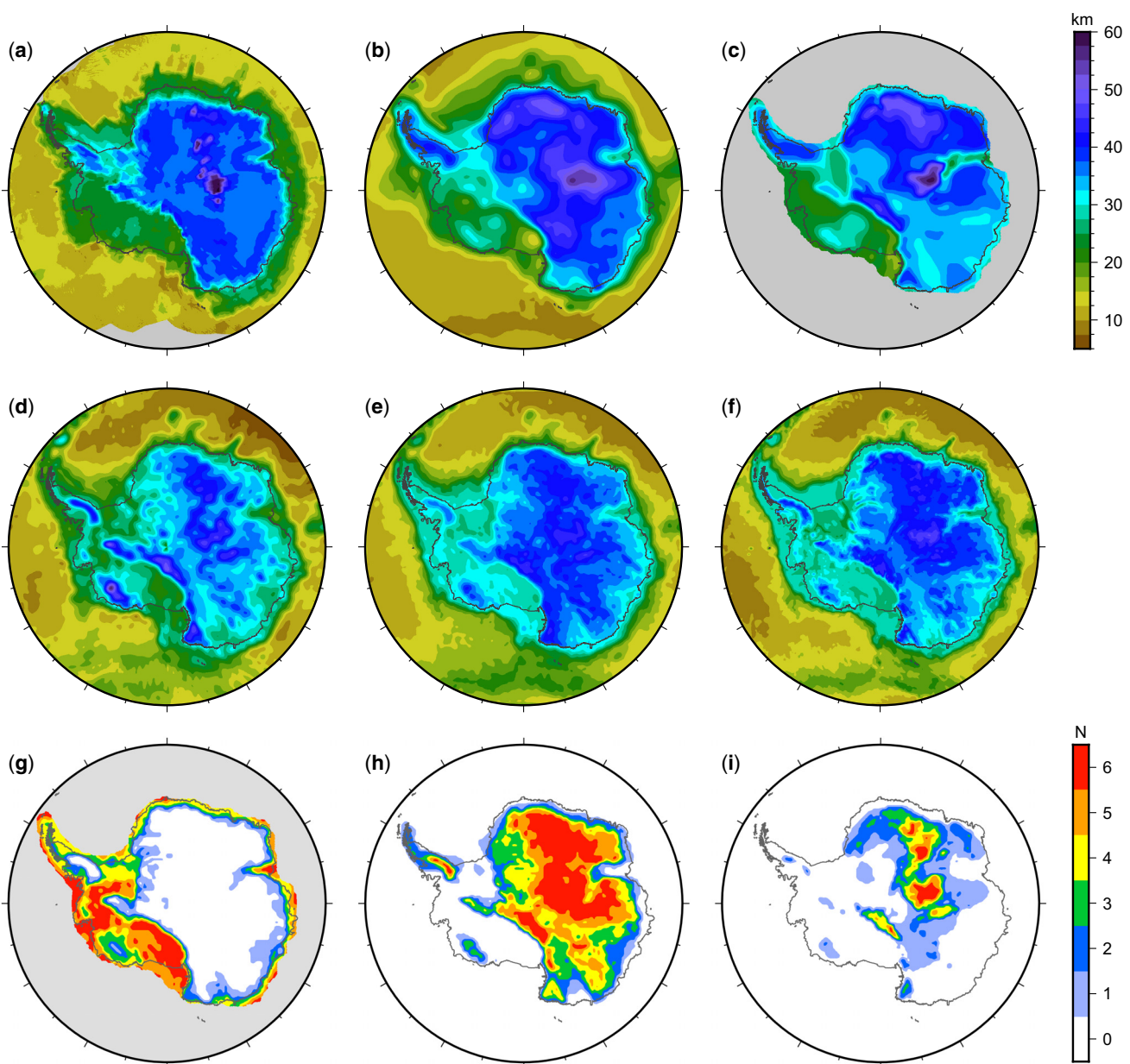


Fig. 3. (a–f) Moho depth models derived with different methods: (a) surface wave analysis, AN1-Moho ([An et al. 2015b](#)); (b) kriging interpolation of local seismologically derived Moho depth estimates filled with estimates from the AN1-Moho model ([Haeger et al. 2019](#)); (c) integrating seismic estimates, gravity data and isostasy ([Baranov et al. 2018](#)); (d) inversion of GOCE gravity gradient data, GEMMA ([Reguzzoni and Sampietro 2015](#)); (e) gravity inversion constrained with seismic estimates ([Pappa et al. 2019a](#)); (f) Airy-isostatic Moho depth model ([Pappa et al. 2019a](#)). (g–i) Vote-maps for different depth ranges illustrate the degree of agreement of the above models: (g) less than 30 km Moho depth; (h) more than 35 km; (i) more than 40 km. Colours indicate the numbers of models that agree for this depth range. For example, reddish areas show high agreement for a shallow Moho in the West Antarctic Rift System (g), whereas only a few spots exist in East Antarctica (i) where all models see a >40 km thick crust.

lithospheric mantle densities, potentially indicating a rock composition depleted in iron. Notwithstanding the poor data situation, the authors were able to show that large parts of East Antarctica's lithospheric mantle are likely strongly depleted in iron and thus enriched in magnesium (Fig. 4), indicated by a high magnesium number ($Mg\# = 100 Mg/(Mg + Fe)$), which suggests cratonic settings of Proterozoic to Archean age. The fact, however, that different up-to-date seismological tomography models lead to inconsistent results in the inversion process demonstrates the need for further field campaigns to collect data, which will enable us to establish more robust models of Antarctica's lithospheric structure.

In order to investigate the characteristics of the upper mantle with gravity modelling, crustal corrections are commonly applied (e.g. [Kaban et al. 2010](#); [Haeger et al. 2019](#)), which

often rely on seismological models. If, however, a trade-off between crustal density, Moho geometry and mantle density is allowed in the modelling (e.g. [Aitken et al. 2013](#)), a reasonably consistent lithospheric model can be established with (partly) sparse seismic coverage. If, in contrast, a fixed crustal density and thickness model derived from seismic findings alone is used as a correction for gravity data, the potential errors in the gravity signal are likely larger than the gravity signal from mantle density variations. Such a seismologically derived crustal model should – if at all – be used extremely cautiously in gravity modelling. As long as the seismic findings considering the thickness and the density of the Antarctic crust remain ambiguous and, in consequence, seismological models cannot provide the degree of certainty required for gravity modelling, other strategies must be pursued in order

Interpretation and modelling of geophysical data

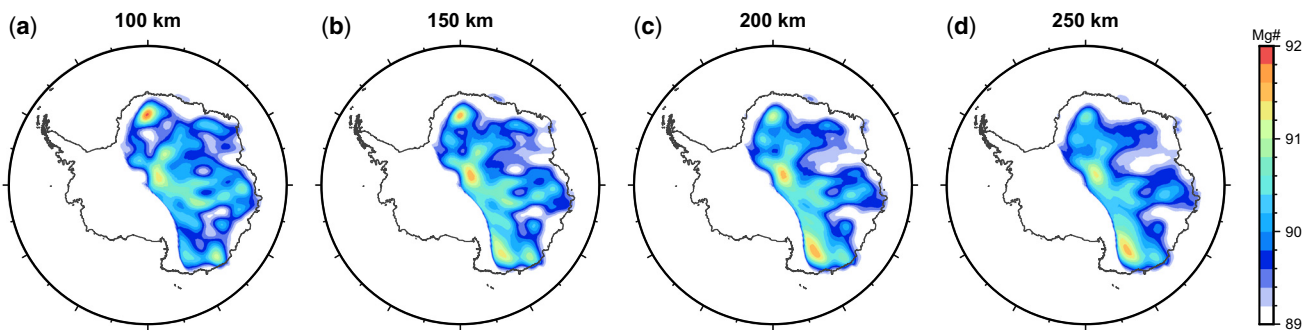


Fig. 4. Depletion variations in terms of Mg# estimated for (a) 100 km, (b) 150 km, (c) 200 km and (d) 250 km, based on the seismic S-wave velocity model SL2013sv (Schaeffer and Lebedev 2013) (after Haeger *et al.* 2019).

to investigate the architecture of the Antarctic lithosphere. One possibility is to model the lithosphere as a whole while considering all those parameters and processes that determine the observables for which data are available. For instance, the temperature strongly affects rock densities due to thermal expansion, the stable mineral assemblage, and the elastic behaviour and thus seismic velocities. Correspondingly, the thermal field of the lithosphere can reasonably be computed by solving the heat transfer equation, whereas the gravity field resulting from the modelled densities and the seismic velocities can be compared with measured data.

Despite the advantages, it is still necessary to make *a priori* assumptions about some parameters like crustal and mantle

rock compositions, which are poorly explored or unknown for large parts of Antarctica. For establishing a lithospheric model of Antarctica, Pappa *et al.* (2019b) relied on petrological studies to define broad regions of different tectonothermal age (Fig. 5a), which were associated with varying degrees of depletion of lithospheric mantle composition. According to the pressure and temperature conditions inside the model, the stable mineral phases (and thus the density) of the respective peridotitic composition were inferred through the thermodynamic modelling software *Perple_X* (Connolly 2005). This method allows modelling of *in situ* densities for rocks under certain assumptions, such as the oxides considered in the system (in this case mantle rocks in the CaO–FeO–MgO–Al₂O₃–

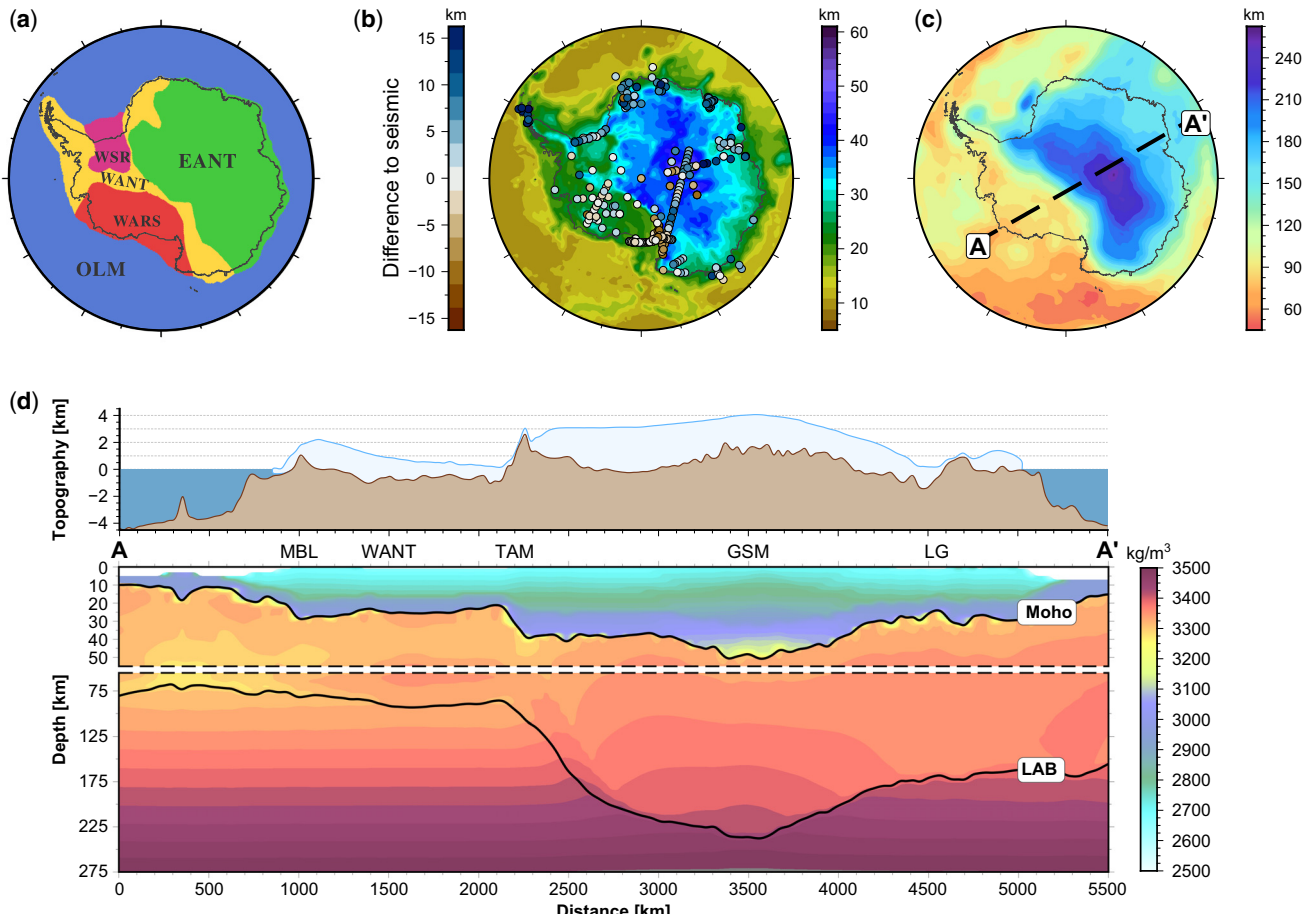


Fig. 5. (a) Domains of different lithospheric mantle composition in the model from Pappa *et al.* (2019b). (b) Resulting Moho depth with local seismic estimates as benchmark (coloured circles and left colour-bar). (c) Resulting total lithospheric thickness. (d) Density cross-section from A–A' (location on (c)). EANT, East Antarctica; GSM, Gamburtsev Subglacial Mountains; LAB, lithosphere–asthenosphere boundary; LG, Lambert Graben; MBL, Marie Byrd Land; OLM, oceanic lithospheric mantle; TAM, Transantarctic Mountains; WANT, West Antarctica; WARS, West Antarctic Rift System; WSR, Weddell Sea Rift.

SiO_2 system). The variety of modelled mineral phases is thus naturally limited. Additionally, representative global values were taken for crustal density and thermal parameters. With this initial set-up, the model was iteratively fitted to the observed topography by maintaining isostatic equilibrium and the satellite gravity gradient data measured by GOCE, always maintaining internal consistency in the relationships between all model properties. The main results of this study are new estimates of the Moho depth and the total lithospheric thickness of Antarctica (**Fig. 5b and c**).

Local seismic Moho depth estimates can serve as *a posteriori* benchmarks instead of using them as an input or constraint as described above. Since the density contrast at the Moho discontinuity in the lithospheric model is a function of temperature, pressure and rock properties, it can vary freely, which leads to a generally good fit of both the gravity gradient data and the seismic Moho depth estimates. In particular, the crustal root beneath the GSM is deeper (*c.* 54 km) in this model than in classical gravity inversions and has a high density of $>3150 \text{ kg m}^{-3}$. A very small density contrast in this region was previously suggested by other studies (Ferraccioli *et al.* 2011; An *et al.* 2015b). The modelled total lithospheric thickness is largely similar to seismological estimates (An *et al.* 2015a) and likewise exhibits a stark contrast between thin lithosphere (*c.* 80 km) in West Antarctica and up to 260 km in East Antarctica. Having such a temperature model of the crust and upper mantle at hand, which agrees with topographic (isostatic), seismic and gravity gradient data, offers the opportunity to derive upper mantle viscosities (Pappa *et al.* 2019b). Especially in Antarctica, it is crucial to consider the three-dimensional variations of viscosity instead of using 1D models (Nield *et al.* 2018; Whitehouse *et al.* 2019) in estimating the glacial isostatic behaviour of the solid Earth, e.g. present-day uplift rates due to ice mass changes.

Magnetic data

Magnetic observations: scales and strides

Antarctica is covered by a number of aeromagnetic surveys as well as satellite magnetic models. Global models derived from single-satellite data have been obtained with accuracies better than a few nanotesla, but rather low resolution due to the dynamic behaviour of the external field, which strongly affects the measurements. The Earth's magnetic field has internal as well as external dynamic sources. Both vary over a wide range of time scales and separating them relies on their different temporal variations. Data from satellite missions have a uniform global coverage but are limited in their spatial resolution by the high altitudes. To distinguish variations in the

lithospheric field from time-dependent contributions of the magnetosphere and ionosphere is especially challenging in polar regions (Langel and Hinze 1998).

A number of global magnetic satellite models have been released since the Ørsted satellite mission was launched in 1999 and joined by the CHAMP satellite mission in 2000. These satellites in low-Earth orbit provide the most effective means of mapping the long wavelengths of the magnetic field caused by the magnetization of the Earth's crust. For instance, the MF6 model was produced using the latest three years of measurements from the CHAMP flux-gate magnetometer (Maus *et al.* 2008). MF6 resolves the crustal magnetic field to spherical harmonic degree 120, corresponding to length scales down to 333 km. The follow-up model MF7 provided the crustal magnetic field to spherical harmonic degree 133, corresponding to length scales down to 300 km (Maus 2010).

In 2013, the Swarm satellite mission, a constellation of three satellites in three different polar orbits was launched. The satellites are located in two orbits, two as a pair in a lower orbit and one upper orbit, between 400 and 550 km altitude. One of the aims is to measure the lithospheric magnetic field to a resolution of 200 km. By combining the measurements of the strength and direction of the magnetic field, the vertical and horizontal derivatives can be calculated, which are less sensitive to time-dependent contributions of the magnetosphere and ionosphere (Kotsiaros and Olsen 2012) and therefore aid in the construction of lithospheric anomalies as in the model LCS-1 (**Fig. 6a**, Olsen *et al.* 2017). The model is improved in comparison to previous models (which were in good agreement up to around SH degree 85, i.e. down to 470 km wavelength); the lithospheric field contribution is now given from spherical harmonic degree 15 to 180 (*c.* 200 km length scales), but satellite data only constrain the part to spherical harmonic degree 135 (*c.* 300 km length scales). For the higher spectral range to degree 180, a certain correlation has been found with the Australian aeromagnetic compilation (Olsen *et al.* 2017). However, in polar regions, the noise to external field sources is significantly higher, making this part, before further detailed examination and validation, unreliable. As for all models, the spherical harmonic degrees up to degree 15 are omitted as this part is dominated by the normal, core field (ranging at the surface from 30 000 nT at the equator to 65 000 nT in polar regions), which masks the lithospheric field contribution.

In order to derive total magnetic field anomalies, called lithospheric magnetic anomalies, from aeromagnetic data, a reference field is subtracted from the measured field representing the normal core field. Routinely, the International Geomagnetic Reference Field (IGRF) for a certain epoch is used. The IGRF is a prediction of the behaviour of the magnetic normal field for an epoch of 5 years (e.g. Thébault *et al.* 2015) and has, especially for Antarctica, a low precision before the onset of satellite measurements. The Definitive Geomagnetic

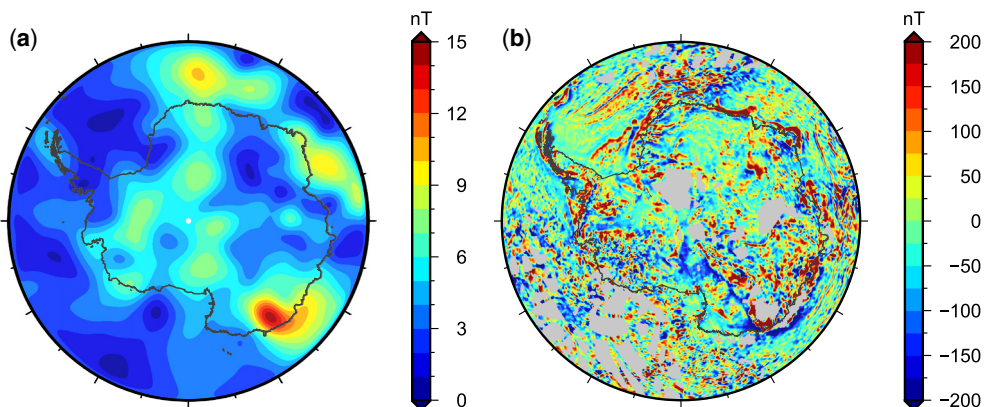


Fig. 6. Lithospheric magnetic anomaly of Antarctica: (a) satellite model LCS-1 (Olsen *et al.* 2017) defined at 400 km height; (b) ADMAP-2 compilation Golynsky *et al.* (2018) based on all available airborne surveys.

Interpretation and modelling of geophysical data

Reference Field (DGRF) is defined for these epochs based on the actual measurements, but data are seldom reprocessed to account for this, when this becomes available. Differences between IGRF and DGRF range in magnitude from 5 to 10 nT, which is low compared to the magnetic normal field, but can be high compared to lithospheric anomalies.

Between satellite and aeromagnetic data, a spectral gap still exists, which hopefully will be smaller with increasing lifetime of the Swarm mission, but also relates to the specifics of aeromagnetic surveys. The first controlling factor for aeromagnetic surveys is the extension, which is usually not larger than a few hundred kilometres. As seen in Figure 6b, Antarctica has an extensive coverage with aeromagnetic surveys and only a few gaps exist. However, the surveys have been acquired over a time-span of more than 50 years and can be divided in quality by data acquired before and after the availability of GPS for navigation (Golynsky *et al.* 2018). Flight lines before GPS have a relatively high uncertainty in navigation as other means have been used for referencing, for example topographic maps, while for later surveys the accuracy is relatively high. Inherent in aeromagnetic surveys is a low precision for the long-wavelength component. That relates to the size of the survey and routine processing techniques, e.g. correction for the reference field (IGRF/DGRF), levelling of datasets, diurnal correction and merging of individual surveys (e.g. Reeves 2005).

Levelling of the flight accounts for varying conditions during flight time such as diurnal variations (short-scale variations of the magnetic field) or varying altitude of the survey. Diurnal variations relate to changes in the magnetic field due to external sources, e.g. sometimes observable as polar lights. To correct for these time-varying effects, a survey has typically normal flight lines and orthogonal tie-lines of 2–5 times the spacing of the normal lines. Between lines and tie-lines, the difference is calculated at the cross-points and these differences are (after an outlier correction) distributed over the survey. After such statistical levelling, in compilations like ADMAP-2 (Golynsky *et al.* 2018) the individual surveys are merged, hereby correcting for the possible shifts in reference level and/or adjusting trends between the surveys. For Antarctic surveys, such a survey configuration has not always been possible as multiple data, which all have individual survey requirements, are acquired at the same time (e.g. Aitken *et al.* 2014; Paxman *et al.* 2019b). In such cases, the data are often filtered to a signal that corresponds to flight lines or can be levelled towards a regional or satellite grid, when available. However, here the spectral content of the data should overlap. All of these corrections do not exclude the overall usability for geological interpretation and affect mostly the long wavelengths (Golynsky *et al.* 2018). The ADMAP-2

compilation provides the most complete and coherent view of the magnetic properties of the Antarctic crust (Fig. 6).

Comparison between the satellite and aeromagnetic data (Fig. 6b) shows that the aeromagnetic surveys are able to image fine-scale crustal properties, while satellite data only provide an image of the broad-scale lithospheric properties, which is often omitted in geological interpretation. Aeromagnetic surveys often lack the long-wavelength component if the extension is not large enough. However, by processing steps affecting the trend, an artificial signal can easily be added unintentionally. Gaina *et al.* (2011) discuss the effect of replacing the long-wavelength component in aeromagnetic surveys by different bandwidth satellite data and show that the effect is significant and that, consequently, only satellite data can be analysed for the long-wavelength behaviour of the field.

Characterization of the magnetic lithosphere

With respect to the sources of the magnetic anomalies, the ADMAP-2 compilation reveals a wide variation of magnetic anomalies reflecting crustal terranes of different lithologies, ages, degrees of tectonic reworking and thermal attributes. The compilation also helps to map out Proterozoic–Archean cratons, Proterozoic–Paleozoic mobile belts, Paleozoic–Cenozoic magmatic arc systems, the boundary between East and West Antarctica, continent–ocean transitions and other regional Antarctic crustal features (Figs 6 and 7, Wilson and Ferraccioli this volume).

Figure 7 shows some examples of data products that can illuminate lithospheric properties. Interpretations of the sources of the magnetic anomalies are often carried out for smaller regions and on the survey-scale, often in combination with gravity analysis (e.g. Ferraccioli *et al.* 2009; Aitken *et al.* 2014). One method to help compare the sources of the gravity and magnetic field is to calculate the pseudo-gravity by applying the Poisson theorem (Blakely 1996). By converting the magnetic anomaly to a corresponding gravity anomaly, short-wavelength features are suppressed and the regional, large-scale features are enhanced. For example, the different characteristics of the West and East Antarctica lithosphere are now easily seen and can be used for further interpretation of the sub-glacial geology. Comparison to the gravity field allows discussion of whether the magnetic and gravity field have the same geological structure as source or, when anomalies do not correlate, whether they are only appearing in one of the datasets. For example, thick sedimentary sequences might not have a clear density contrast to the surrounding bedrock due to the sedimentary density increase with depth but will have a magnetic signature due to sedimentary rocks

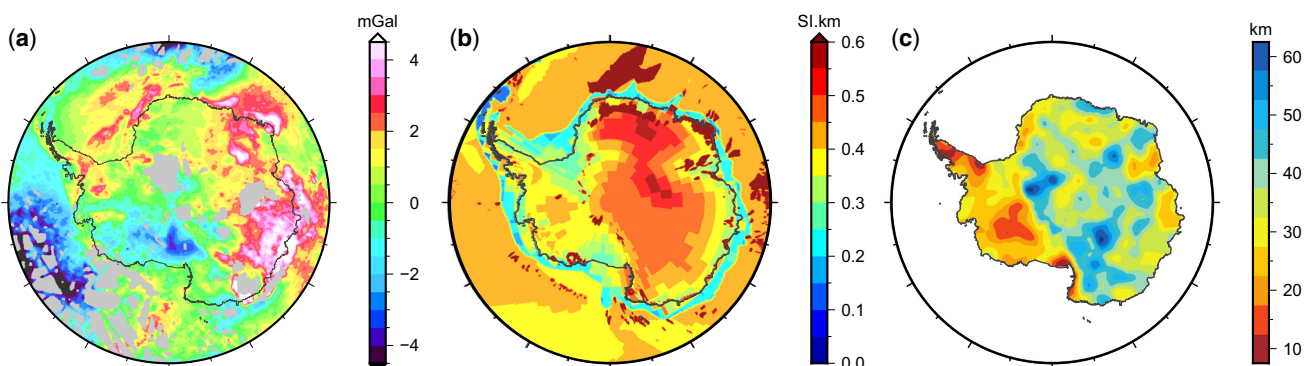


Fig. 7. Characteristics of the magnetic lithosphere: (a) pseudo-gravity calculated from ADMAP-2; (b) susceptibility of the lithosphere after the VIS model from Hemant and Maus (2005); (c) depth to deepest magnetic sources, after Martos *et al.* (2017).

typically having low magnetization relative to basement rocks, and are often regarded as magnetically transparent.

One of the few maps of lithospheric magnetization covering the Antarctic continent is presented by [Hemant and Maus \(2005\)](#). In their global study, the vertically integrated susceptibility (VIS) is calculated based on geological and tectonic maps of the world, laboratory susceptibility values of the occurring rock types and the seismic thickness of the crust. Unfortunately, the results for Antarctica reveal the poor quality and absence of such information and show the need to establish a database of rock properties to be able to update such products.

A different approach is not to invert for magnetization, but to estimate the deepest magnetic sources by assuming a piecewise constant susceptibility. This is of particular interest as the deepest sources can be associated with the depth to the Curie isotherm, hereby defining a thermal boundary. The Curie temperature of a ferromagnetic material is the temperature where the material loses its characteristic ferromagnetic ability: the ability to possess a net and spontaneous magnetization in the presence of an external inducing magnetic field. Rocks at higher temperatures will not generate a discernible magnetic signal. Magnetite, with a Curie temperature of 580°C (e.g. [Hunt et al. 1995](#)), is regarded as the dominant magnetic mineral in crustal rocks, while the Curie temperatures for felsic plutonic rocks can range from 400 to 550°C, related to variability in composition of titanomagnetites between substantially different rock types (e.g. basalt v. granite, [Byerly and Stolt 1977](#)). In most stable continental areas this temperature range includes the lower crust or upper mantle (e.g. [McKenzie et al. 2005](#)), although often the Moho depth is defined as a maximum depth for the Curie isotherm ([Wasilewski and Mayhew 1992](#)). However, at the Moho depth, temperatures might be well below the 580°C isotherm, especially in areas of tectonothermal cold cratons like East Antarctica. This implies that even the upper mantle can be magnetized, although the amplitudes of magnetization might be low.

[Ferré et al. \(2014\)](#) summarized a number of reasons why magnetization in the upper mantle might be reasonable, even though the classical view is that there is a lack of magnetic rocks in the mantle (e.g. [Wasilewski and Mayhew 1992](#)). [Idoko et al. \(2019\)](#) demonstrated by forward modelling based on assumed geotherms, the pressure dependence of the Curie temperature of magnetite, and the statistical distributions of rock magnetic data from mantle xenoliths, that the upper mantle magnetization potentially contributes up to 10% of the observed long-wavelength lithospheric magnetic anomalies.

In Antarctica, [Fox Maule et al. \(2005\)](#) and [Martos et al. \(2017\)](#) presented geothermal heat flow models based on analysis of magnetic data. [Fox Maule et al. \(2005\)](#) used one of the first magnetic satellite models (from the Ørsted mission) to

calculate the deepest magnetic sources using some specific boundary conditions, for example a susceptibility of 0.035 (SI) and 0.040 (SI) for the continental and oceanic crust, respectively. The magnetic field used is filtered by spherical harmonic degree 14, as the lower spherical harmonic degrees are dominated by the core field. To circumvent this, the long-wavelength part of their model is taken from a crustal thickness model ([Nataf and Ricard 1996](#)), which is based on seismic and thermal data. This study was followed up by [Martos et al. \(2017\)](#), using ADMAP-1 ([Golynksy et al. 2001](#)) plus some additional new aeromagnetic surveys and by filling the gaps with satellite data. More specifically, the long-wavelength content (>150 km) of all aeromagnetic data was filtered and replaced with the satellite model MF7 ([Maus 2010](#)). In the characteristic power-spectrum, parts of the spectrum can be associated with a certain source depth, which can be estimated from the slope of the curve (e.g. [Spector and Grant 1970](#); [Tanaka et al. 1999](#)). In their study, [Martos et al. \(2017\)](#) pre-defined a characteristic wavelength range both for East and West Antarctica separately, to calculate for a window size of 350 km the depth to the magnetic sources. Due to use of the window size, the results have to be treated carefully in areas where only satellite data are used as these are only reliable for a signal with wavelengths beyond 300 km.

Both the approach by [Fox Maule et al. \(2005\)](#) and [Martos et al. \(2017\)](#) assume a constant magnetization with depth, and [Fox Maule et al. \(2005\)](#) exclude depths larger than the Moho depth from a seismic model. [Figure 7c](#) shows the deepest magnetic sources from the analysis of [Martos et al. \(2017\)](#), which shows depths of more than 40 km in East Antarctica and areas of relatively shallow magnetic source depth in West Antarctica. Inversions of magnetic data to find the deepest magnetic source have been attempted previously in regions other than Antarctica in a number of studies (e.g. [Bouligand et al. 2009](#); [Ebbing et al. 2009](#); [Tanaka 2017](#)). Both [Bouligand et al. \(2009\)](#) and [Ebbing et al. \(2009\)](#) compared such depth estimates with thermal and structural information and discussed the uncertainties resulting, for example, from the fact that the deepest magnetic sources could be related to structural boundaries in the crust and not represent the depth of the Curie isotherm. Similar interpretations could be made for Antarctica using the pseudo-gravity map ([Fig. 7a](#)), which shows similar domains as the gravity field, since both the magnetization contrast and the geometry influence the magnetic field anomalies.

All this considered, at least in areas where the deepest magnetic source is located beneath the Moho depth, such depth estimates must be treated with care. In [Figure 8b](#), we have therefore clipped the deepest magnetic sources for areas where they are located beneath the Moho depth. Somewhat surprisingly, the deepest magnetic sources are hereby clipped for half of the continent, indicating that a more complex magnetization model has to be developed in the future to address

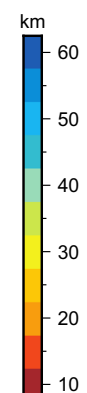
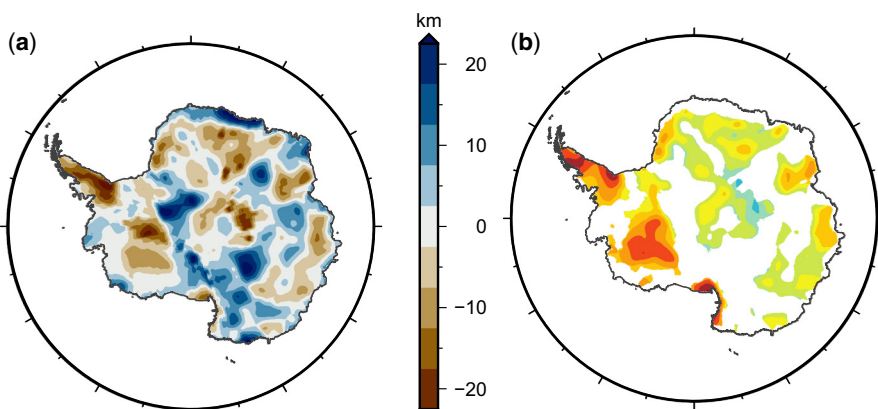


Fig. 8. (a) Difference between the depth to the deepest magnetic sources ([Fig. 7c; Martos et al. 2017](#)) and the crustal thickness ([Fig. 3a; An et al. 2015b](#)). (b) The deepest magnetic sources clipped for areas where the model is located beneath the Moho depth.

Interpretation and modelling of geophysical data

both the lateral and vertical variations in the magnetic parameters.

Antarctic magnetic data in a Gondwana framework

An application where magnetic data are often used is in linking Antarctica to its neighbours in a Gondwana framework. An example is shown in Figure 9 with the datasets of southern Africa, Antarctica and Australia. For example, Finn *et al.* (1999) and Aitken *et al.* (2014, 2016) use such reconstructions to discuss the structural setting of East Antarctica with respect to the structural setting of southern Australia and show that the magnetic data indicate the continuation of Australia under the ice of Antarctica. Similar studies have been carried out for other parts of Gondwana by Mieth and Jokat (2014), Ruppel *et al.* (2018) and Mueller and Jokat (2019).

Plate tectonic reconstructions have also been used by Pollett *et al.* (2019) to derive information on the thermal structure of Antarctica by interpolating thermal parameters from adjacent continents into Antarctica.

Geothermal heat flow

A short summary of models

The thermal structure of the continent is one of the most unknown parameters of Antarctica, but is critical for a variety of applications on different scales, e.g. ice-sheet modelling or glacial-isostatic adjustment (e.g. Burton-Johnson *et al.* 2020*a*, *b*). Despite some drilling initiatives, the remoteness and vastness of the continent limits the possibilities to achieve a good, homogeneous coverage of the entire continent for thermal information. Only very sparse heat flow measurements have been taken in boreholes into sub-glacial lake sediments (e.g. Fisher *et al.* 2015) or seafloor sedimentary strata (e.g. Schröder

et al. 2011) or derived from basal temperature gradients in deep ice boreholes (e.g. Engelhardt 2004). Some of the recent drilling initiatives have measured values $>120 \text{ mW m}^{-2}$ in West Antarctica, far exceeding the heat flow normally measured over the continental crust. Such a high heat flow, if existing on a regional scale, is clearly a boundary condition that has to be considered in ice-sheet dynamics but might also indicate a thin and subsequently warm lithosphere, which might imply low viscosity influencing glacial isostatic adjustment.

A number of geothermal heat flow models are available for Antarctica as discussed in Van Liefferinge *et al.* (2018) and Burton-Johnson *et al.* (2020*a*). These models are derived from geophysical data that indirectly reflect the thermal structure and vary largely (Fig. 10). A full review of the data and models is provided in the two recent white papers from Burton-Johnson *et al.* (2020*a, b*), but in the absence of homogeneous coverage with heat flow measurements, different means have to be used. Pollett *et al.* (2019) assessed the heat flow over Antarctica by kriging interpolation of existing heat flow measurements, making use of the heat flow data of the continents adjacent to Antarctica. A motivation of the study was the disagreement of the existing models.

Magnetic analysis (e.g. Fox Maule *et al.* 2005; Martos *et al.* 2017) relies on estimates of the deepest magnetic source and has large uncertainty where the magnetic data quality is low and/or where the assumptions of a simple magnetic layer are not met. From the deepest sources the heat flow is then calculated by applying a one-dimensional thermal model assuming constant thermal parameters. Fox Maule *et al.* (2005) themselves estimate the error in their map of sub-glacial heat flow to be in the range of $21\text{--}27 \text{ mW m}^{-2}$, due to the limited resolution of a few hundred kilometres of the existing magnetic data (resulting from the satellite altitude), methodological uncertainties with associated errors and the use of a laterally constant crustal heat production. Martos *et al.* (2017) provide a considerably lower uncertainty based on their approach, which is, however, only valid where aeromagnetic survey data are used and the magnetic depth is not beneath

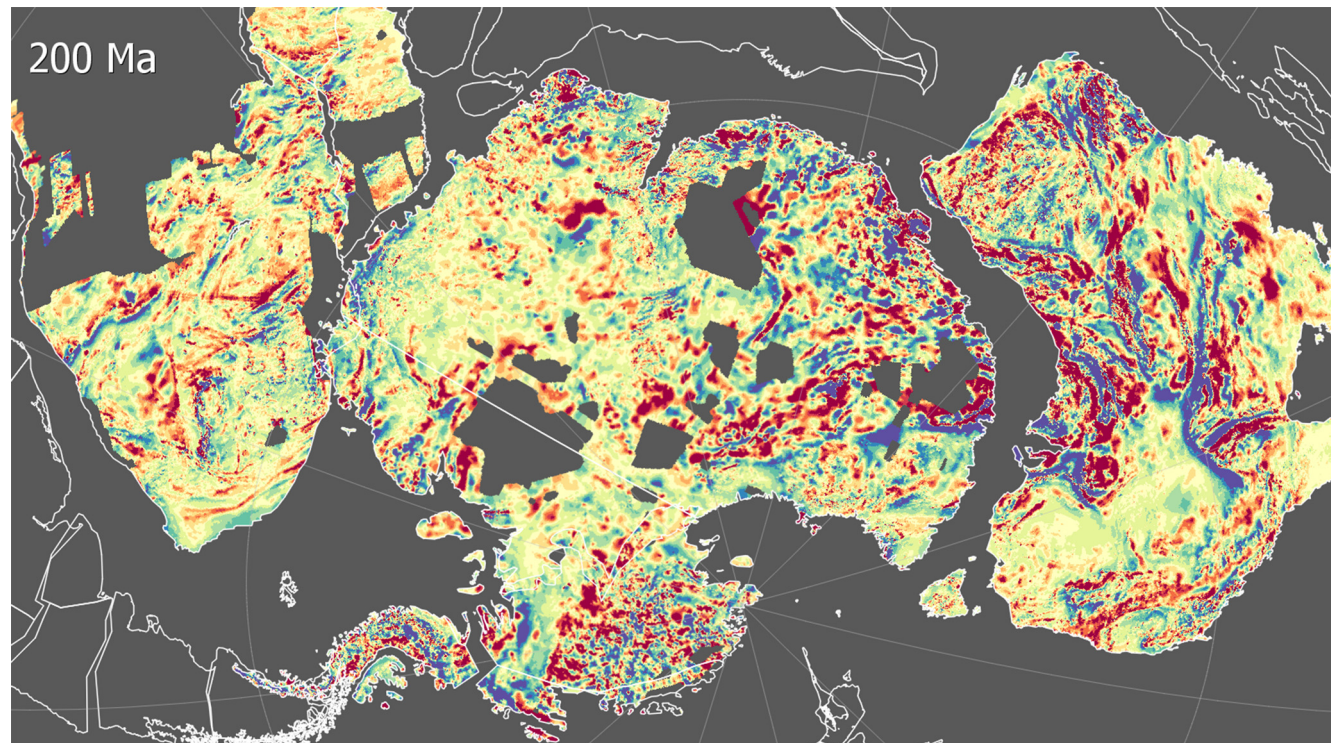


Fig. 9. Gondwana reconstruction of aeromagnetic anomaly maps. The datasets shown are the aeromagnetic compilations of South Africa (Stettler *et al.* 2000), Australia (Milligan *et al.* 2004) and ADMAP-2 (Golynsky *et al.* 2018) after conformation to the satellite model LCS-1.

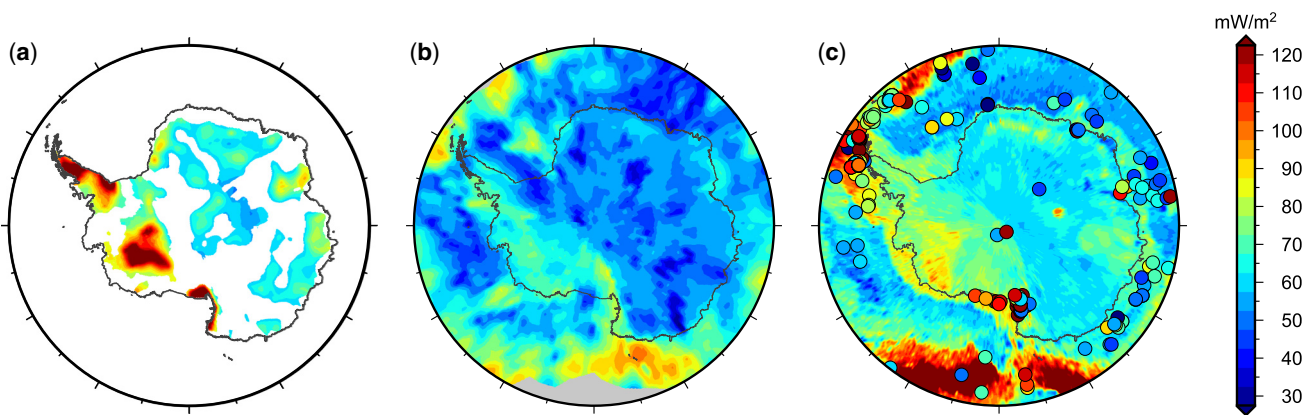


Fig. 10. Heat flow models for Antarctica: (a) Martos *et al.* (2017) clipped for areas, where the estimated deepest magnetic source is located beneath the Moho depth (compare Fig. 8b); (b) An *et al.* (2015a); (c) Lucaleau (2019) with measurements.

the Moho depth. In general, such estimates mainly reflect the changes in crustal properties.

Due to the absence of near-surface measurements and the uncertainties in magnetic data interpretation, heat flow has been alternatively determined from seismic data (e.g. Shapiro and Ritzwoller 2004; An *et al.* 2015a; Shen *et al.* 2020). Assuming that temperature is the dominant control on seismic velocity in the upper mantle, the temperature field in the lithosphere can be determined and with some assumptions the geothermal heat flow can be estimated. With an estimate of lithospheric heat production rates, a map of the sub-glacial heat flow can be produced. However, these models are also limited to a lateral resolution of >120 km and are insensitive to the lithospheric geotherm. Also, the lithosphere is treated as internally laterally uniform in its structure (only varying in thickness) and possessing low and homogeneous radiogenic heat production. Consequently, sub-glacial heat flow inversely correlates with lithospheric thickness with the highest values overlying the thinnest lithosphere.

Similar to this, Pappa *et al.* (2019b) estimated geothermal heat flow based on gravity modelling in combination with seismological constraints. These heat flow models, however, do not reflect small-scale patterns caused by variations in hydrothermal circulation, volcanic activity or crustal radioactive heat production, but mostly provide an assessment of the background heat flow from the mantle and an extrapolation of such values to the surface by assuming constant crustal parameters. A different approach is used by Macelloni *et al.* (2018) based on SMOS satellite data, who inverted geothermal heat flow against ice temperature profiles based on radar data. However, this approach requires specific boundary conditions such as thick ice cover and is therefore only valid in central East Antarctica. That explains some of the reasons for the differences between the heat flow models in Figure 10.

To complicate the situation, Burton-Johnson *et al.* (2017) showed for the Antarctic Peninsula that the upper crust can contribute up to 70% to the geothermal heat flow. Therefore, models of geothermal heat flow should utilize a heterogeneous upper crust with variable radioactive heat production rates if they are to predict basal conditions of the ice-sheet accurately.

Alternative approaches have been proposed, for example machine learning (e.g. Rezvanbehbahani *et al.* 2017) or similarity methods (e.g. Lucaleau 2019). In both methods, a large number of geophysical models and geological data are used to statistically predict heat flow in areas of sparse measurement coverage. Both approaches are hereby first tested in areas where heat flow is known with relatively low uncertainty and later on applied to remote areas. In Figure 10c, the model from Lucaleau (2019) is shown derived as part of his

new global heat flow model based on empirical correlations between geophysical and geological datasets. Such analysis can be done in a Gondwana framework to provide further input to derive the geothermal heat flow for East Antarctica. An example of this is Pollett *et al.* (2019), who assessed the heat flow over Antarctica by kriging interpolation of existing heat flow measurements of Antarctica and adjacent continents.

There is still significant disagreement between current geothermal heat flow models. Lösing *et al.* (2020) analysed with Bayesian inversion the trade-offs between the different geophysical parameters and showed that the current models cannot be reconciled within a plausible parameter range. However, that would be crucial in order to provide a useful assessment as input for modelling of Antarctic ice stream behaviour. For Greenland, Rogozhina *et al.* (2012) estimated the effect of such differences in geothermal heat flow models on the evolution of the Greenland ice-sheet. In summary, they concluded that the uncertainties of the geophysical models prohibit their use for ice-sheet modelling and that instead a constant heat-flow value provides a considerably better fit with the majority of the observational data. Yet, there is no geothermal heat flow model available for Antarctica to overcome this limitation.

Conclusions

A wealth of gravity and magnetic data from airborne surveys and satellite missions is available for Antarctica. While airborne data cover about two-thirds of the continent, their resolution and accuracy is variable. Satellite data offer homogeneous accuracy and limited resolution to help fill the gaps in airborne data, and aid interpretation of the lithospheric architecture. Satellite data, in combination with airborne data, or on their own, can be used to illuminate the structure, thermal state and composition of the lithosphere, especially when combined with seismological information. Studies based on these datasets agree with seismological data on the overall architecture of the Antarctic mantle and highlight the differences between East and West Antarctica in lithospheric thickness, mantle composition and geothermal heat flow. East Antarctica is cratonic, but the degree of complexity is modelled differently between recent studies (e.g. Ebbing *et al.* 2018; Haeger *et al.* 2019; Pappa *et al.* 2019a, b). Similar debates are ongoing for the makeup of West Antarctica. Gravity data can aid in testing competing hypotheses, while the magnetic data can provide details of the crustal configuration.

Interpretation and modelling of geophysical data

Geophysical models on scales relevant to understanding the dynamics of ice sheets can be improved by more detailed petrophysical information. This has worked well elsewhere, for example in Scandinavia Olesen *et al.* (2010) showed a susceptibility map based on rock measurements averaged over geological units aided interpretation and modelling. An important application of this in Antarctica is in understanding geo-thermal heat flow, which, on a local scale, is dominated by the thermal conductivity and heat production in the crust. Pollett *et al.* (2019) demonstrated how heat flow parameters can be used in a Gondwana framework, which for East Antarctica adds information from the adjacent continents of South Africa, India and Australia which could be better guided by incorporating geophysical data interpretation and petrophysical data. In this way, the different thermal history of the lithosphere after break-up could be considered, as could the interaction of the asthenosphere and lithosphere (see Bredow and Steinberger 2021, Wiens this volume in review, Hu *et al.* 2018).

Burton-Johnson *et al.* (2020b) summarized the challenges in providing accurate geothermal heat flow models with associated uncertainties and recommended future research directions. Coupled with modern approaches such as machine learning, one will be able to probe a wider range of geological and geophysical proxies to establish consistent integrated geo-physical–petrological models of the solid Earth part of Antarctica. This is in line with the conclusions by Kennicutt *et al.* (2019) who summarized the need for improving and consolidating solid Earth studies in Antarctica. Both the need for multi-technique analyses combining seismological, petrological and potential field data has been expressed as well as open access to data and models to enhance our understanding of Antarctica.

Acknowledgements The authors thank Alan R.A. Aitken and one anonymous reviewer as well as the editors Wouter van der Wal and Adam P. Martin for their constructive contribution and criticism.

Author contributions FP: conceptualization (supporting), resources (equal), writing – original draft (equal), writing – review & editing (equal); **JE:** conceptualization (equal), methodology (lead), resources (equal), writing – original draft (equal), writing – review & editing (equal).

Funding This study was supported by the European Space Agency ESA by funding the projects GOCE + Antarctica and 3D Earth within the Support to Science Element (STSE) programme.

Data availability Data sharing is not applicable to this article as no datasets were generated or analysed during the current study.

References

- Aitken, A.R.A., Salmon, M.L. and Kennett, B.L.N. 2013. Australia's Moho: a test of the usefulness of gravity modelling for the determination of Moho depth. *Tectonophysics*, **609**, 468–479, <https://doi.org/10.1016/j.tecto.2012.06.049>
- Aitken, A.R.A., Young, D.A. *et al.* 2014. The subglacial geology of Wilkes Land, East Antarctica. *Geophysical Research Letters*, **41**, 2390–2400, <https://doi.org/10.1002/2014GL059405>
- Aitken, A.R.A., Betts, P.G., Young, D.A., Blankenship, D.D., Roberts, J.L. and Siegert, M.J. 2016. The Australo-Antarctic Columbia to Gondwana transition. *Gondwana Research*, **29**, 136–152, <https://doi.org/10.1016/j.gr.2014.10.019>
- An, M., Wiens, D.A. *et al.* 2015a. Temperature, lithosphere–asthenosphere boundary, and heat flux beneath the Antarctic Plate inferred from seismic velocities. *Journal of Geophysical Research: Solid Earth*, **120**, 8720–8742, <https://doi.org/10.1002/2015JB011917>
- An, M., Wiens, D.A. *et al.* 2015b. S-velocity model and inferred Moho topography beneath the Antarctic Plate from Rayleigh waves. *Journal of Geophysical Research: Solid Earth*, **120**, 359–383, <https://doi.org/10.1002/2014JB011332>
- An, M., Wiens, D.A. and Zhao, Y. 2016. A frozen collision belt beneath ice: an overview of seismic studies around the Gamburtsev Subglacial Mountains, East Antarctica. *Advances in Polar Science*, **27**, 78–89, <https://doi.org/10.13679/j.advp.2016.2.00078>
- Artemieva, I.M., Thybo, H. and Cherepanova, Y. 2019. Isopycnicity of cratonic mantle restricted to kimberlite provinces. *Earth and Planetary Science Letters*, **505**, 13–19, <https://doi.org/10.1016/j.epsl.2018.09.034>
- Bamber, J.L., Ferraccioli, F., Joughin, I., Shepherd, T., Rippin, D.M., Siegert, M.J. and Vaughan, D.G. 2006. East Antarctic ice stream tributary underlain by major sedimentary basin. *Geology*, **34**, 33–36, <https://doi.org/10.1130/G22160.1>
- Baranov, A. and Morelli, A. 2013. The Moho depth map of the Antarctica region. *Tectonophysics*, **609**, 299–313, <https://doi.org/10.1016/j.tecto.2012.12.023>
- Baranov, A., Tenzer, R. and Bagherbandi, M. 2018. Combined gravimetric–seismic crustal model for Antarctica. *Surveys in Geophysics*, **39**, 23–56, <https://doi.org/10.1007/s10712-017-9423-5>
- Barzaghi, R., Betti, B., Carrion, D., Gentile, G., Maseroli, R. and Sacerdote, F. 2014. Orthometric correction and normal heights for Italian levelling network: a case study. *Applied Geomatics*, **6**, 17–25, <https://doi.org/10.1007/s12518-013-0121-9>
- Bell, R.E., Ferraccioli, F. *et al.* 2011. Widespread persistent thickening of the East Antarctic Ice Sheet by freezing from the base. *Science*, **331**, 1592–1595, <https://doi.org/10.1126/science.1200109>
- Blakely, R.J. 1996. *Potential Theory in Gravity and Magnetic Applications*. Cambridge University Press.
- Block, A.E., Bell, R.E. and Studinger, M. 2009. Antarctic crustal thickness from satellite gravity: implications for the Transantarctic and Gamburtsev Subglacial Mountains. *Earth and Planetary Science Letters*, **288**, 194–203, <https://doi.org/10.1016/j.epsl.2009.09.022>
- Bouligand, C., Glen, J.M.G. *et al.* 2009. Mapping Curie temperature depth in the western United States with a fractal model for crustal magnetization. *Journal of Geophysical Research*, **114**, B11104, <https://doi.org/10.1029/2008JD011281>
- Bouman, J., Ebbing, J. *et al.* 2015. GOCE gravity gradient data for lithospheric modeling. *International Journal of Applied Earth Observation and Geoinformation*, **35**, 16–30, <https://doi.org/10.1016/j.jag.2013.11.001>
- Bouman, J., Ebbing, J. *et al.* 2016. Satellite gravity gradient grids for geophysics. *Scientific Reports*, **6**, 21050, <https://doi.org/10.1038/srep21050>
- Bredow, E. and Steinberger, B. 2021. Mantle convection and possible mantle plumes beneath Antarctica: insights from geodynamic models and implications for topography. *Geological Society, London, Memoirs*, **56**, <https://doi.org/10.1144/M56-2020-2>
- Brockmann, J.M., Zehentner, N., Höck, E., Pail, R., Loth, I., Mayer-Gürr, T. and Schuh, W.-D. 2014. EGM_TIM_RL05: an independent geoid with centimeter accuracy purely based on the GOCE mission. *Geophysical Research Letters*, **41**, 8089–8099, <https://doi.org/10.1002/2014GL061904>
- Burton-Johnson, A., Halpin, J.A., Whittaker, J.M., Graham, F.S. and Watson, S.J. 2017. A new heat flux model for the Antarctic Peninsula incorporating spatially variable upper crustal radiogenic heat production. *Geophysical Research Letters*, **44**, 5436–5446, <https://doi.org/10.1002/2017GL073596>
- Burton-Johnson, A., Dziadek, R. and Martin, C. 2020a. Geothermal heat flow in Antarctica: current and future directions. *The Cryosphere Discussions*, <https://doi.org/10.5194/tc-2020-59>

- Burton-Johnson, A., Dziadek, R. and The SERCE Geothermal Heat Flow Sub-Group 2020b. Antarctic Geothermal Heat Flow: Future research directions. White Paper, <https://www.scar.org/scar-news/serce-news/scar-serce-ghf/>
- Byerly, P. and Stolt, R. 1977. An attempt to define the Curie point isotherm in northern and central Arizona. *Geophysics*, **42**, 1394–1400, <https://doi.org/10.1190/1.1440800>
- Cammarano, F., Goes, S., Vacher, P. and Giardini, D. 2003. Inferring upper-mantle temperatures from seismic velocities. *Physics of the Earth and Planetary Interiors*, **138**, 197–222, [https://doi.org/10.1016/S0031-9201\(03\)00156-0](https://doi.org/10.1016/S0031-9201(03)00156-0)
- Chaput, J., Aster, R.C. et al. 2014. The crustal thickness of West Antarctica. *Journal of Geophysical Research: Solid Earth*, **119**, 378–395, <https://doi.org/10.1002/2013JB010642>
- Chen, B., Haeger, C., Kaban, M.K. and Petrunin, A.G. 2018. Variations of the effective elastic thickness reveal tectonic fragmentation of the Antarctic lithosphere. *Tectonophysics*, **746**, 412–424, <https://doi.org/10.1016/j.tecto.2017.06.012>
- Connolly, J.A.D. 2005. Computation of phase equilibria by linear programming: a tool for geodynamic modeling and its application to subduction zone decarbonation. *Earth and Planetary Science Letters*, **236**, 524–541, <https://doi.org/10.1016/j.epsl.2005.04.033>
- Eaton, D.W. and Perry, H.K.C. 2013. Ephemeral isopycnicity of cratonic mantle keels. *Nature Geoscience*, **6**, 967, <https://doi.org/10.1038/ngeo1950>
- Eaton, D.W., Darbyshire, F., Evans, R.L., Grüter, H., Jones, A.G. and Yuan, X. 2009. The elusive lithosphere–asthenosphere boundary (LAB) beneath cratons. *Lithos*, **109**, 1–22, <https://doi.org/10.1016/j.lithos.2008.05.009>
- Ebbing, J., Gernigon, L., Pascal, C., Olesen, O. and Osmundsen, P.T. 2009. A discussion of structural and thermal control of magnetic anomalies on the mid-Norwegian margin. *Geophysical Prospecting*, **57**, 665–681, <https://doi.org/10.1111/j.1365-2478.2009.00800.x>
- Ebbing, J., Haas, P., Ferraccioli, F., Pappa, F., Szwilus, W. and Bouman, J. 2018. Earth tectonics as seen by GOCE - Enhanced satellite gravity gradient imaging. *Scientific Reports*, **8**, 16356, <https://doi.org/10.1038/s41598-018-34733-9>
- Engelhardt, H. 2004. Thermal regime and dynamics of the West Antarctic ice sheet. *Annals of Glaciology*, **39**, 85–92, <https://doi.org/10.3189/172756404781814203>
- Ferraccioli, F., Armadillo, E., Jordan, T., Bozzo, E. and Corr, H. 2009. Aeromagnetic exploration over the East Antarctic Ice Sheet: a new view of the Wilkes Subglacial Basin. *Tectonophysics*, **478**, 62–77, <https://doi.org/10.1016/j.tecto.2009.03.013>
- Ferraccioli, F., Finn, C.A., Jordan, T.A., Bell, R.E., Anderson, L.M. and Damaske, D. 2011. East Antarctic rifting triggers uplift of the Gamburtsev Mountains. *Nature*, **479**, 388–392, <https://doi.org/10.1038/nature10566>
- Ferré, E.C., Friedman, S.A. et al. 2014. Eight good reasons why the uppermost mantle could be magnetic. *Tectonophysics*, **624–625**, 3–14, <https://doi.org/10.1016/j.tecto.2014.01.004>
- Filina, I.Y., Blankenship, D.D., Thoma, M., Lukin, V.V., Masolov, V.N. and Sen, M.K. 2008. New 3D bathymetry and sediment distribution in Lake Vostok: implication for pre-glacial origin and numerical modeling of the internal processes within the lake. *Earth and Planetary Science Letters*, **276**, 106–114, <https://doi.org/10.1016/j.epsl.2008.09.012>
- Finn, C., Moore, D., Damaske, D. and Mackey, T. 1999. Aeromagnetic legacy of early Paleozoic subduction along the Pacific margin of Gondwana. *Geology*, **27**, 1087–1090, [https://doi.org/10.1130/0091-7613\(1999\)027<1087:ALOEPS>2.3.CO;2](https://doi.org/10.1130/0091-7613(1999)027<1087:ALOEPS>2.3.CO;2)
- Fisher, A.T., Mankoff, K.D. et al. 2015. High geothermal heat flux measured below the West Antarctic Ice Sheet. *Science Advances*, **1**, e1500093, <https://doi.org/10.1126/sciadv.1500093>
- Forsberg, R. 2015. GOCE and Antarctica. In: *5th International GOCE User Workshop*. ESA Special Publication, 3.
- Forsberg, R., Olesen, A., Yıldız, H. and Tscherning, C.C. 2011. Polar Gravity Fields from GOCE and Airborne Gravity. In: *4th International GOCE User Workshop*. ESA Special Publication, 8.
- Forsberg, R., Olesen, A.V. et al. 2018. Exploring the Recovery Lakes region and interior Dronning Maud Land, East Antarctica, with airborne gravity, magnetic and radar measurements. *Geological Society, London, Special Publications*, **461**, 23–34, <https://doi.org/10.1144/SP461.17>
- Fox Maule, C., Purucker, M.E., Olsen, N. and Mosegaard, K. 2005. Heat flux anomalies in Antarctica revealed by satellite magnetic data. *Science*, **309**, 464–467, <https://doi.org/10.1126/science.1106888>
- Frederick, B.C., Young, D.A., Blankenship, D.D., Richter, T.G., Kempf, S.D., Ferraccioli, F. and Siegert, M.J. 2016. Distribution of subglacial sediments across the Wilkes Subglacial Basin, East Antarctica. *Journal of Geophysical Research: Earth Surface*, **121**, 790–813, <https://doi.org/10.1002/2015JF003760>
- Fretwell, P., Pritchard, H.D. et al. 2013. Bedmap2: improved ice bed, surface and thickness datasets for Antarctica. *The Cryosphere*, **7**, 375–393, <https://doi.org/10.5194/tc-7-375-2013>
- Fullea, J., Afonso, J.C., Connolly, J.A.D., Fernández, M., García-Castellanos, D. and Zeyen, H. 2009. LitMod3D: an interactive 3-D software to model the thermal, compositional, density, rheological and seismological structure of the lithosphere and sublithospheric upper mantle. *Geochemistry, Geophysics, Geosystems*, **10**, <https://doi.org/10.1029/2009GC002391>
- Fullea, J., Lebedev, S., Agius, M.R., Jones, A.G. and Afonso, J.C. 2012. Lithospheric structure in the Baikal–central Mongolia region from integrated geophysical-petrological inversion of surface-wave data and topographic elevation. *Geochemistry, Geophysics, Geosystems*, **13**, <https://doi.org/10.1029/2012GC004138>
- Gaina, C., Werner, S.C., Saltus, R. and Maus, S. 2011. Circum-Arctic mapping project: new magnetic and gravity anomaly maps of the Arctic. *Geological Society, London, Memoirs*, **35**, 39–48, <https://doi.org/10.1144/M35.3>
- Golynsky, A., Chiappini, M. et al. 2001. ‘ADMAP – Magnetic Anomaly Map of the Antarctic,’ 1:10 000 000 scale map. In: Morris, P. and von Frese, R. (eds) *BAS (Misc.)*. British Antarctic Survey, Cambridge, 10.
- Golynsky, A.V., Ferraccioli, F. et al. 2018. New magnetic anomaly map of the Antarctic. *Geophysical Research Letters*, **45**, 6437–6449, <https://doi.org/10.1029/2018GL078153>
- Haeger, C. and Kaban, M.K. 2019. Decompensative gravity anomalies reveal the structure of the upper crust of Antarctica. *Pure and Applied Geophysics*, **176**, 4401–4414, <https://doi.org/10.1007/s00024-019-02212-5>
- Haeger, C., Kaban, M.K., Tesauro, M., Petrunin, A.G. and Mooney, W.D. 2019. 3-D density, thermal, and compositional model of the Antarctic lithosphere and implications for its evolution. *Geochemistry, Geophysics, Geosystems*, **20**, 688–707, <https://doi.org/10.1029/2018GC008033>
- Hansen, S.E., Nyblade, A.A., Heeszel, D.S., Wiens, D.A., Shore, P. and Kanao, M. 2010. Crustal structure of the Gamburtsev Mountains, East Antarctica, from S-wave receiver functions and Rayleigh wave phase velocities. *Earth and Planetary Science Letters*, **300**, 395–401, <https://doi.org/10.1016/j.epsl.2010.10.022>
- Hansen, S.E., Kenyon, L.M., Graw, J.H., Park, Y. and Nyblade, A.A. 2016. Crustal structure beneath the Northern Transantarctic Mountains and Wilkes Subglacial Basin: implications for tectonic origins. *Journal of Geophysical Research: Solid Earth*, **121**, 812–825, <https://doi.org/10.1002/2015JB012325>
- Harrowfield, M., Holdgate, G.R., Wilson, C.J.L. and McLoughlin, S. 2005. Tectonic significance of the Lambert graben, East Antarctica: reconstructing the Gondwanan rift. *Geology*, **33**, 197–200, <https://doi.org/10.1130/G21081.1>
- Hemant, K. and Maus, S. 2005. Geological modeling of the new CHAMP magnetic anomaly maps using a geographical information system technique. *Journal of Geophysical Research: Solid Earth*, **110**, <https://doi.org/10.1029/2005JB003837>
- Hu, J., Liu, L., Faccenda, M., Zhou, Q., Fischer, K.M., Marshak, S. and Lundstrom, C. 2018. Modification of the Western Gondwana craton by plume–lithosphere interaction. *Nature Geoscience*, **11**, 203–210, <https://doi.org/10.1038/s41561-018-0064-1>

Interpretation and modelling of geophysical data

- Hunt, C.P., Moskowitz, B.M., Banerjee, S.K. 1995. Magnetic properties of rocks and minerals. In: Ahrens, T.J. (ed.) *Rock Physics and Phase Relations. A Handbook of Physical Constants*. American Geophysical Union, 189–204.
- Idoko, C.M., Conder, J.A., Ferré, E.C. and Filiberto, J. 2019. The potential contribution to long wavelength magnetic anomalies from the lithospheric mantle. *Physics of the Earth and Planetary Interiors*, **292**, 21–28, <https://doi.org/10.1016/j.pepi.2019.05.002>
- Isanina, E.V., Krupnova, N.A., Popov, S.V., Masolov, V.N. and Lukin, V.V. 2009. Deep structure of the Vostok Basin, East Antarctica as deduced from seismological observations. *Geotectonics*, **43**, 221–225, <https://doi.org/10.1134/S0016852109030042>
- Jordan, T., Ferraccioli, F. et al. 2017. First complete regional view of the Pensacola-Pole Basin from PolarGAP radar data. *EGU General Assembly Conference Abstracts*, Vienna, Austria, 15902.
- Jordan, T.H. 1988. Structure and formation of the continental tectosphere. *Journal of Petrology, Special_Volume*, 11–37, https://doi.org/10.1093/petrology/Special_Volume.1.11
- Kaban, K.M., Schwintzer, P. and Reigber, C.H. 2004. A new isostatic model of the lithosphere and gravity field. *Journal of Geodesy*, **78**, 368–385, <https://doi.org/10.1007/s00190-004-0401-6>
- Kaban, M.K., Schwintzer, P., Artemieva, I.M. and Mooney, W.D. 2003. Density of the continental roots: compositional and thermal contributions. *Earth and Planetary Science Letters*, **209**, 53–69, [https://doi.org/10.1016/S0012-821X\(03\)00072-4](https://doi.org/10.1016/S0012-821X(03)00072-4)
- Kaban, M.K., Tesauro, M. and Cloetingh, S.A.P.L. 2010. An integrated gravity model for Europe's crust and upper mantle. *Earth and Planetary Science Letters*, **296**, 195–209, <https://doi.org/10.1016/j.epsl.2010.04.041>
- Karner, G.D., Studinger, M. and Bell, R.E. 2005. Gravity anomalies of sedimentary basins and their mechanical implications: application to the Ross Sea basins, West Antarctica. *Earth and Planetary Science Letters*, **235**, 577–596, <https://doi.org/10.1016/j.epsl.2005.04.016>
- Kennicutt, M.C. II, Bromwich, D. et al. 2019. Sustained Antarctic Research: a 21st century imperative. *One Earth*, **1**, 95–113, <https://doi.org/10.1016/j.oneear.2019.08.014>
- Kotsiaros, S. and Olsen, N. 2012. The geomagnetic field gradient tensor. *GEM. International Journal on Geomathematics*, **3**, 297–314, <https://doi.org/10.1007/s13137-012-0041-6>
- Krupnik, I., Allison, I. et al. (eds) 2011. *Understanding Earth's Polar Challenges: International Polar Year 2007–2008*, CCI Press, Edmonton, Alberta and University of the Arctic, Rovaniemi, Finland (printed version) and ICSU/WMO Joint Committee for International Polar Year 2007–2008.
- Langel, R.A. and Hinze, W.J. 1998. *The Magnetic Field of the Earth's Lithosphere: The Satellite Perspective*. Cambridge University Press.
- Lawrence, J.F., Wiens, D.A., Nyblade, A.A., Anandakrishnan, S., Shore, P.J. and Voigt, D. 2006. Rayleigh wave phase velocity analysis of the Ross Sea, Transantarctic Mountains, and East Antarctica from a temporary seismograph array. *Journal of Geophysical Research: Solid Earth*, **111**, <https://doi.org/10.1029/2005JB003812>
- LeMasurier, W.E. and Rex, D.C. 1989. Evolution of linear volcanic ranges in Marie Byrd Land, West Antarctica. *Journal of Geophysical Research: Solid Earth*, **94**, 7223–7236, <https://doi.org/10.1029/JB094iB06p07223>
- Lisker, F., Prenzel, J., Läufer, A. and Spiegel, C. 2013. The regional thermochronological record as evaluation criterion for uplift models of the Transantarctic Mountains. *EGU General Assembly Conference Abstracts*, EGU2013-5985, Vienna, Austria.
- Lloyd, A.J. 2018. *Seismic Tomography of Antarctica and the Southern Oceans: Regional and Continental Models from the Upper Mantle to the Transition Zone*. Washington University, St. Louis, Missouri.
- Lloyd, A.J., Wiens, D.A. et al. 2015. A seismic transect across West Antarctica: evidence for mantle thermal anomalies beneath the Bentley Subglacial Trench and the Marie Byrd Land Dome. *Journal of Geophysical Research: Solid Earth*, **120**, 8439–8460, <https://doi.org/10.1002/2015JB012455>
- Lösing, M., Ebbing, J. and Szwilus, W. 2020. Geothermal heat flux in antarctica: assessing models and observations by Bayesian inversion. *Frontiers in Earth Science*, **8**, 105, <https://doi.org/10.3389/feart.2020.00105>
- Lucazeau, F. 2019. Analysis and mapping of an updated terrestrial heat flow dataset. *Geochemistry, Geophysics, Geosystems*, **20**, 4001–4024, <https://doi.org/10.1029/2019GC008389>
- Lythe, M.B. and Vaughan, D.G. 2001. BEDMAP: a new ice thickness and subglacial topographic model of Antarctica. *Journal of Geophysical Research: Solid Earth*, **106**, 11335–11351, <https://doi.org/10.1029/2000JB900449>
- Macelloni, G. and Brogioni, M. et al. 2018. Cryorad: a low frequency wideband radiometer mission for the study of the cryosphere. *IGARSS 2018–2018, IEEE International Geoscience and Remote Sensing Symposium*, 1998–2000.
- Martos, Y.M., Catalán, M., Jordan, T.A., Golynsky, A., Golynsky, D., Eagles, G. and Vaughan, D.G. 2017. Heat flux distribution of Antarctica unveiled. *Geophysical Research Letters*, **44**, 11,417–11,426, <https://doi.org/10.1002/2017GL075609>
- Maus, S. 2010. Magnetic field model MF7, <http://geomag.org/models/MF7.html>
- Maus, S., Yin, F. et al. 2008. Resolution of direction of oceanic magnetic lineations by the sixth-generation lithospheric magnetic field model from CHAMP satellite magnetic measurements. *Geochemistry Geophysics Geosystems*, **9**, Q07021, <https://doi.org/10.1029/2008GC001949>
- Mayer-Gürr, T., Eicker, A., Kurtenbach, E. and Ilk, K.-H. 2010. ITG-GRACE: global static and temporal gravity field models from GRACE data. In: Flechtner, F.M., Gruber, T., Güntner, A., Mandea, M., Rothacher, M., Schöne, T. and Wickert, J. (eds) *System Earth via Geodetic-Geophysical Space Techniques*. Springer, Berlin, 159–168, https://doi.org/10.1007/978-3-642-10228-8_13
- Mayer-Gürr, T., Rieser, D. et al. 2012. The new combined satellite only model GOCO03s. Venice.
- McKenzie, D., Jackson, J. and Priestley, K. 2005. Thermal structure of oceanic and continental lithosphere. *Earth and Planetary Science Letters*, **233**, 337–349, <https://doi.org/10.1016/j.epsl.2005.02.005>
- McKenzie, D., Yi, W. and Rummel, R. 2015. Estimates of Te for continental regions using GOCE gravity. *Earth and Planetary Science Letters*, **428**, 97–107, <https://doi.org/10.1016/j.epsl.2015.07.036>
- Mieth, M. and Jokat, W. 2014. New aeromagnetic view of the geological fabric of southern Dronning Maud Land and Coats Land, East Antarctica. *Gondwana Research*, **25**, 358–367, <https://doi.org/10.1016/j.gr.2013.04.003>
- Milligan, P.R., Franklin, R. and Ravat, D. 2004. A new generation magnetic anomaly grid database of Australia (MAGDA). *Preview*, **113**, 25–29.
- Mishra, D.C., Sekhar, D.V.C., Raju, D.C.V. and Kumar, V.V. 1999. Crustal structure based on gravity-magnetic modelling constrained from seismic studies under Lambert Rift, Antarctica and Godavari and Mahanadi rifts, India and their interrelationship. *Earth and Planetary Science Letters*, **172**, 287–300, [https://doi.org/10.1016/S0012-821X\(99\)00212-5](https://doi.org/10.1016/S0012-821X(99)00212-5)
- Moritz, H. 1990. The inverse Vening Meinesz problem in isostasy. *Geophysical Journal International*, **102**, 733–738, <https://doi.org/10.1111/j.1365-246X.1990.tb04591.x>
- Morlighem, M., Rignot, E. et al. 2020. Deep glacial troughs and stabilizing ridges unveiled beneath the margins of the Antarctic ice sheet. *Nature Geoscience*, **13**, 132–137, <https://doi.org/10.1038/s41561-019-0510-8>
- Mueller, C.O. and Jokat, W. 2019. The initial Gondwana break-up: a synthesis based on new potential field data of the Africa–Antarctica Corridor. *Tectonophysics*, **750**, 301–328, <https://doi.org/10.1016/j.tecto.2018.11.008>
- Nataf, H.-C. and Ricard, Y. 1996. 3SMAC: an a priori tomo graphic model of the upper mantle based on geophysical modeling. *Physics of the Earth and Planetary Interiors*, **95**, 101–122, [https://doi.org/10.1016/0031-9201\(95\)03105-7](https://doi.org/10.1016/0031-9201(95)03105-7)
- Nield, G.A., Whitehouse, P.L., van der Wal, W., Blank, B., O'Donnell, J.P. and Stuart, G.W. 2018. The impact of lateral variations

- in lithospheric thickness on glacial isostatic adjustment in West Antarctica. *Geophysical Journal International*, **214**, 811–824, <https://doi.org/10.1093/gji/ggy158>
- Nowell, D.A.G. 1999. Gravity terrain corrections – an overview. *Journal of Applied Geophysics*, **42**, 117–134, [https://doi.org/10.1016/S0926-9851\(99\)00028-2](https://doi.org/10.1016/S0926-9851(99)00028-2)
- O'Donnell, J.P. and Nyblade, A.A. 2014. Antarctica's hypsometry and crustal thickness: implications for the origin of anomalous topography in East Antarctica. *Earth and Planetary Science Letters*, **388**, 143–155, <https://doi.org/10.1016/j.epsl.2013.11.051>
- Oldenburg, D.W. 1974. The inversion and interpretation of gravity anomalies. *Geophysics*, **39**, 526–536, <https://doi.org/10.1190/1.1440444>
- Olesen, O. and Brönnér, M. *et al.* 2010. New aeromagnetic and gravity compilations from Norway and adjacent areas: methods and applications. *Geological Society, London, Petroleum Geology Conference Series*, **7**, 559, <https://doi.org/10.1144/0070559>
- Olsen, N., Ravat, D., Finlay, C.C. and Kother, L.K. 2017. LCS-1: a high-resolution global model of the lithospheric magnetic field derived from CHAMP and Swarm satellite observations. *Geophysical Journal International*, **211**, 1461–1477, <https://doi.org/10.1093/gji/ggx381>
- Pail, R., Fecher, T., Barnes, D., Factor, J.F., Holmes, S.A., Gruber, T. and Zingerle, P. 2018. Short note: the experimental geopotential model XGM2016. *Journal of Geodesy*, **92**, 443–451, <https://doi.org/10.1007/s00190-017-1070-6>
- Pappa, F., Ebbing, J. and Ferraccioli, F. 2019a. Moho depths of antarctica: comparison of seismic, gravity, and isostatic results. *Geochemistry, Geophysics, Geosystems*, **20**, 1629–1645, <https://doi.org/10.1029/2018GC008111>
- Pappa, F., Ebbing, J., Ferraccioli, F. and van der Wal, W. 2019b. Modeling satellite gravity gradient data to derive density, temperature, and viscosity structure of the antarctic lithosphere. *Journal of Geophysical Research: Solid Earth*, **124**, 12053–12076, <https://doi.org/10.1029/2019JB017997>
- Parker, R.L. 1973. The rapid calculation of potential anomalies. *Geophysical Journal International*, **31**, 447–455, <https://doi.org/10.1111/j.1365-246X.1973.tb06513.x>
- Paxman, G.J. 2021. Antarctic palaeotopography. *Geological Society, London, Memoirs*, **56**, <https://doi.org/10.1144/M56-2020-7>
- Paxman, G.J., Jamieson, S.S., Ferraccioli, F., Bentley, M.J., Ross, N., Watts, A.B., ... and Young, D.A. 2019a. The role of lithospheric flexure in the landscape evolution of the Wilkes Subglacial Basin and Transantarctic Mountains, East Antarctica. *Journal of Geophysical Research: Earth Surface*, **124**, 812–829, <https://doi.org/10.1029/2018JF004705>
- Paxman, G.J., Jamieson, S.S. *et al.* 2019b. Subglacial geology and geomorphology of the Pensacola-Pole Basin, East Antarctica. *Geochemistry, Geophysics, Geosystems*, **20**, 2786–2807, <https://doi.org/10.1029/2018GC008126>
- Peidou, A. and Pagiatakis, S. 2019. Gravity gradiometry with GRACE space missions: new opportunities for the geosciences. *Journal of Geophysical Research: Solid Earth*, **124**, 9130–9147, <https://doi.org/10.1029/2018JB016382>
- Pollett, A., Hasterok, D., Raimondo, T., Halpin, J.A., Hand, M., Bendall, B. and McLaren, S. 2019. Heat flow in Southern Australia and connections with East Antarctica. *Geochemistry, Geophysics, Geosystems*, **20**, <https://doi.org/10.1029/2019GC008418>
- Rabbel, W., Kaban, M. and Tesauro, M. 2013. Contrasts of seismic velocity, density and strength across the Moho. *Tectonophysics*, **609**, 437–455, <https://doi.org/10.1016/j.tecto.2013.06.020>
- Ramirez, C., Nyblade, A. *et al.* 2016. Crustal and upper-mantle structure beneath ice-covered regions in Antarctica from S-wave receiver functions and implications for heat flow. *Geophysical Journal International*, **204**, 1636–1648, <https://doi.org/10.1093/gji/ggv542>
- Reeves, C. 2005. Aeromagnetic surveys: principles, practice and interpretation. *Geosoft*, **155**.
- Reguzzoni, M. and Sampietro, D. 2015. GEMMA: an Earth crustal model based on GOCE satellite data. *International Journal of Applied Earth Observation and Geoinformation*, **35**, 31–43, <https://doi.org/10.1016/j.jag.2014.04.002>
- Reigber, C. 2006. A high resolution global gravity field model combining CHAMP and GRACE satellite mission and surface data: EIGEN-CG01C. *Scientific Technical Report*, Geoforschungszentrum Potsdam, <https://doi.org/10.23689/fidgeo-564>
- Rezvanbehbahani, S., Stearns, L.A., Kadivar, A., Walker, J.D. and van der Veen, C.J. 2017. Predicting the geothermal heatflux in Greenland: a machine learning approach. *Geophysical Research Letters*, **44**, 12,271–12,279, <https://doi.org/10.1002/2017GL075661>
- Riedel, S., Jokat, W. and Steinlage, D. 2012. Mapping tectonic provinces with airborne gravity and radar data in Dronning Maud Land, East Antarctica. *Geophysical Journal International*, **189**, 414–427, <https://doi.org/10.1111/j.1365-246X.2012.05363.x>
- Rogozhina, I., Hagedoorn, J.M., Martinec, Z., Fleming, K., Soucek, O., Greve, R. and Thomas, M. 2012. Effects of uncertainties in the geothermal heat flux distribution on the Greenland Ice Sheet: an assessment of existing heat flow models. *Journal of Geophysical Research*, **117**, F02025, <https://doi.org/10.1029/2011JF002098>
- Rummel, R., Yi, W. and Stummer, C. 2011. GOCE gravitational gradiometry. *Journal of Geodesy*, **85**, 777, <https://doi.org/10.1007/s00190-011-0500-0>
- Ruppel, A., Jacobs, J., Eagles, G., Läufer, A. and Jokat, W. 2018. New geophysical data from a key region in East Antarctica: estimates for the spatial extent of the Tonian Oceanic Arc Super Terrane (TOAST). *Gondwana Research*, **59**, 97–107, <https://doi.org/10.1016/j.gr.2018.02.019>
- Schaeffer, A.J. and Lebedev, S. 2013. Global shear speed structure of the upper mantle and transition zone. *Geophysical Journal International*, **194**, 417–449, <https://doi.org/10.1093/gji/ggt095>
- Scheinert, M., Ferraccioli, F. *et al.* 2016. New Antarctic gravity anomaly grid for enhanced geodetic and geophysical studies in Antarctica. *Geophysical Research Letters*, **43**, 600–610, <https://doi.org/10.1002/2015GL067439>
- Schröder, H., Paulsen, T. and Wonik, T. 2011. Thermal properties of the AND-2A borehole in the southern Victoria Land Basin, McMurdo Sound, Antarctica. *Geosphere*, **7**, 1324–1330, <https://doi.org/10.1130/GES00690.1>
- Sebera, J., Haagmans, R., Floberghagen, R. and Ebbing, J. 2018. Gravity spectra from the density distribution of Earth's uppermost 435 km. *Surveys in Geophysics*, **39**, 227–244, <https://doi.org/10.1007/s10712-017-9445-z>
- Shapiro, N.M. and Ritzwoller, M.H. 2004. Inferring surface heat flux distributions guided by a global seismic model: particular application to Antarctica. *Earth and Planetary Science Letters*, **223**, 213–224, <https://doi.org/10.1016/j.epsl.2004.04.011>
- Shen, W., Wiens, D.A. *et al.* 2018. The crust and upper mantle structure of central and West Antarctica from Bayesian inversion of Rayleigh Wave and Receiver Functions. *Journal of Geophysical Research: Solid Earth*, **123**, 7824–7849, <https://doi.org/10.1029/2017JB015346>
- Shen, W., Wiens, D.A., Lloyd, A.J. and Nyblade, A.A. 2020. A geothermal heat flux map of Antarctica empirically constrained by seismic structure. *Geophysical Research Letters*, **47**, e2020GL086955, <https://doi.org/10.1029/2020GL086955>
- Shephard, G.E., Matthews, K.J., Hosseini, K. and Domeier, M. 2017. On the consistency of seismically imaged lower mantle slabs. *Scientific Reports*, **7**, 10976, <https://doi.org/10.1038/s41598-017-11039-w>
- Spector, A. and Grant, F.S. 1970. Statistical models for interpreting aeromagnetic data. *Geophysics*, **35**, 293–302, <https://doi.org/10.1190/1.1440092>
- Stern, T.A. and ten Brink, U.S. 1989. Flexural uplift of the Transantarctic Mountains. *Journal of Geophysical Research*, **94**, 10315–10330, <https://doi.org/10.1029/JB094iB08p10315>
- Stettler, E.H., Fourie, C.J.S. and Cole, P. 2000. Total magnetic field intensity map of the Republic of South Africa (in 4 panels). *Council for Geoscience, Pretoria*, 2000.

Interpretation and modelling of geophysical data

- Stixrude, L. and Lithgow-Bertelloni, C. 2005. Mineralogy and elasticity of the oceanic upper mantle: origin of the low-velocity zone. *Journal of Geophysical Research: Solid Earth*, **110**, 1978–2012, <https://doi.org/10.1029/2004JB00 2965>
- Straume, E.O., Gaina, C. et al. 2019. GlobSed: updated total sediment thickness in the World's Oceans. *Geochemistry, Geophysics, Geosystems*, **20**, 1756–1772, <https://doi.org/10.1029/2018G C008115>
- Studinger, M., Karner, G.D., Bell, R.E., Levin, V., Raymond, C.A. and Tikku, A.A. 2003. Geophysical models for the tectonic framework of the Lake Vostok region, East Antarctica. *Earth and Planetary Science Letters*, **216**, 663–677, [https://doi.org/10.1016/S0012-821X\(03\)00548-X](https://doi.org/10.1016/S0012-821X(03)00548-X)
- Szwillus, W., Afonso, J.C., Ebbing, J. and Mooney, W.D. 2019. Global crustal thickness and velocity structure from geostatistical analysis of seismic data. *Journal of Geophysical Research: Solid Earth*, **124**, 1626–1652, <https://doi.org/10.1029/2018JB016593>
- Tanaka, A. 2017. Global centroid distribution of magnetized layer from world digital magnetic anomaly map. *Tectonics*, **36**, 3248–3253, <https://doi.org/10.1002/2017TC004770>
- Tanaka, A., Okubo, Y. and Matsubayashi, O. 1999. Curie point depth based on spectrum analysis of the magnetic anomaly data in East and Southeast Asia. *Tectonophysics*, **306**, 461–470, [https://doi.org/10.1016/S0040-1951\(99\)00072-4](https://doi.org/10.1016/S0040-1951(99)00072-4)
- Tapley, B.D., Bettadpur, S., Ries, J.C., Thompson, P.F. and Watkins, M.M. 2004. GRACE measurements of mass variability in the earth system. *Science*, **305**, 503–505, <https://doi.org/10.1126/science.1099192>
- Thébault, E., Finlay, C.C., Alken, P., Beggan, C.D., Canet, E., Chulliat, A. and Rother, M. 2015. Evaluation of candidate geomagnetic field models for IGRF-12. *Earth, Planets and Space*, **67**, 112, <https://doi.org/10.1186/s40623-015-0273-4>
- Van Liefferinge, B., Pattyn, F., Cavitte, M.G.P., Karlsson, N.B., Young, D.A., Sutter, J. and Eisen, O. 2018. Promising Oldest Ice sites in East Antarctica based on thermodynamical modelling. *The Cryosphere*, **12**, 2773–2787, <https://doi.org/10.5194/tc-12-2773-2018>
- Wasilewski, P.J. and Mayhew, M.A. 1992. The Moho as a magnetic boundary revisited. *Geophysical Research Letters*, **19**, 2259–2262, <https://doi.org/10.1029/92GL01997>
- Watts, A.B. 2001. *Isostasy and Flexure of the Lithosphere*. Cambridge University Press.
- Whitehouse, P.L., Gomez, N., King, M.A. and Wiens, D.A. 2019. Solid Earth change and the evolution of the Antarctic Ice Sheet. *Nature Communications*, **10**, 503, <https://doi.org/10.1038/s41467-018-08068-y>
- Wiens, D. this volume, in review. The Seismic Structure of the Antarctic Upper Mantle. *Geological Society, Memoirs*, **56**.
- Yildiz, H., Forsberg, R., Tscherning, C.C., Steinhage, D., Eagles, G. and Bouman, J. 2017. Upward continuation of Dome-C airborne gravity and comparison with GOCE gradients at orbit altitude in east Antarctica. *Studia Geophysica et Geodaetica*, **61**, 53–68, <https://doi.org/10.1007/s11200-015-0634-2>
- Zingerle, P., Pail, R., Scheinert, M. and Schaller, T. 2019. Evaluation of terrestrial and airborne gravity data over Antarctica – a generic approach. *Journal of Geodetic Science*, **9**, 29, <https://doi.org/10.1515/jogs-2019-0004>